Microzooplankton grazing impact on phytoplankton after a storm event in Kane`ohe Bay, O`ahu

A THESIS SUBMITTED TO THE GLOBAL ENVIRONMENTAL SCIENCE UNDERGRADUATE DIVISION IN PARTIAL FULFILLMENT OF THE REQUIREMENTS FOR THE DEGREE OF

BACHELOR OF SCIENCE

IN

GLOBAL ENVIRONMENTAL SCIENCE

DECEMBER 2012

By
Galiel A. Kolker

Thesis Advisor
Karen E. Selph

I certify that I have read this thesis and that, in my opinion, it is satisfactory in scope and quality as a thesis for the degree of Bachelor of Science in Global Environmental Science.

THESIS ADVISOR

_____

Karen E. Selph
Department of Oceanography

ACKNOWLEDGEMENTS

I'd like to extend my thanks to Drs. Erica Goetze, Paul Bienfang and Petra Lenz for their helpful contributions of lab space and equipment, as well as collaboration on this project; to Jane Schoonmaker, for providing guidance along a challenging and rigorous path.

A very special thanks to my exceptional advisor, Dr. Karen E. Selph, whose encouragement, generosity, good sense of humor and expertise made this adventure possible.

ABSTRACT

A relatively new area of research has developed over the past 30 years, that of the microbial food web and the grazing dynamics therein. Microzooplankton (the 20-200 µm size category including copepod nauplii, ciliates, and flagellates) are the principal grazers of phytoplankton. Nanoplankton (2-20 µm) were also included in this study, since they are known to graze picoplankton (0.2-2 µm), the smallest phytoplankton in the microbial food web. Our research focused on the effects the presence or absence of nutrients had on the composition of phytoplankton and grazers in water samples taken in South Kaneohe Bay, near Coconut Island. We sampled storm (KBG1) and non-storm conditions (KBG2), artificially supplementing some samples with nutrients. We used Landry and Hassett's (1982) dilution technique to achieve the desired fraction of whole seawater to filtered seawater, and hence the desired dilution of grazers. We calculated the net phytoplankton growth in storm versus non-storm, in all dilution factors, and with varying additions of nutrients. We observed net phytoplankton growth rates (which includes mortality by microzooplankton) was higher the more diluted (and fewer grazers) there were in our water samples. The doubling rates of phytoplankton growth during storm conditions (KBG1) were largely unaffected by the artificial addition of nutrients, since growth conditions were already optimal due to nutrient loading from input streams following a storm (for example, *Prochlorococcus* doubled abundance in 12.7 hours with added nutrients versus an 11.6-hour doubling rate without added nutrients). For storm conditions, an average of 83% of phytoplankton growth was consumed by grazers, and so net phytoplankton growth was positive. In contrast, the doubling rates were greatly affected by artificial nutrient additions during nutrient-depleted non-storm conditions

(KBG2). Non-storm samples with artificially added nutrients had doubling rates of 2-4x faster (for example, *Prochlorococcus* doubled in abundance in 24.0 hours) than non-storm samples without added nutrients (*Prochlorococcus* doubled in 44.8 hours). For non-storm conditions, grazers consumed an average of 112% of phytoplankton growth, making net phytoplankton growth negative. Our findings agreed with the prior research; that is, non-storm conditions were dominated by the smaller cells, such as *Synechococcus sp.* (0.2-2 μm), and storm conditions were dominated by the larger cells such as chain-forming centric diatoms *Chaetoceros sp.*

TABLE OF CONTENTS **Page**

LIST OF TABLES **Page**

LIST OF FIGURES **Page**

1. INTRODUCTION AND BACKGROUND

1.1. Microzooplankton and the microbial food web

Although 90% of ocean biomass is microbial, the food web dynamics at this level are a relatively new area of research. The past 30 years have been a time of increased attention and study for this complex component of the oceanic food web. Our current understanding of ocean metabolism, based on over 75 years of research in this field, suggests that microbes dominate (Landry, 2002). As pointed out by Fenchel (2008), as early as 1935, Keys et al. questioned the role of protists (single-cell eukaryotes which include heterotrophic grazers and phytoplankton) and whether they controlled bacterial populations in a then-unknown part of the oceanic food web (Fenchel, 2008). This preceded by decades the significant 1983 paper by Azam et al., which brought the concept of the microbial loop to the attention of biological oceanographers as an area where much research was needed.

Before this recent increase in microbial research, it was believed that trophic levels were arranged in a simple, direct, linear chain, from the smallest organisms up to the top predators. With new research, we are learning that the true trophic pathways form more of a web, in which predators find their prey at all different levels of organisms, not just the one directly below the predator, as previously thought.

The linear model of energy transfer was, in order of ascension up the trophic levels: diatoms, copepods, krill, fish, whales. Pomeroy's 1974 review indicated new awareness that our food web included many more components outside this standard sequence of producers and consumers. For example, particulate and dissolved organic matter, zooplankton excretion, bacteria and heterotrophic protists are now understood to

play important roles in the oceanic food web and biogeochemical cycling of matter in the ocean. The main concept Azam et al. (1983) emphasized regarding the microbial loop was that the recycled minerals and nutrients from predation provided feedback to this microbial loop. A diagram of Azam et al.'s microbial loop is presented below, in **Figure 1.** Note in the Azam et al. diagram, the pivotal role of the "phagotrophic protozoa" in connecting the microbial food web to the classic food chain. "Phagotrophic protozoa" are the same microzooplankton protist grazers we are concerned with in this research.

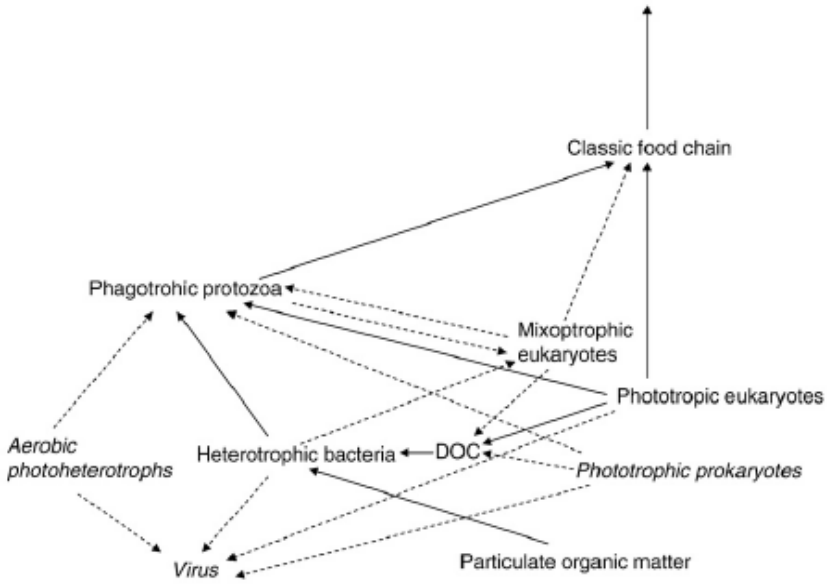

Figure 1. Azam et al.'s (1983) microbial loop, as separate from the classic food chain.

Our current understanding of the basic microbial energy transfer up through trophic levels is: autotrophic bacteria to small heterotrophic protists (flagellates), then to larger protists (ciliates, dinoflagellates), followed by metazoans like copepods, and continuing higher up the trophic levels to fish. It is thought that the interactions between bacteria and flagellates (the smallest of the protists) may account for 44-75% of the energy flux pathway at this level (Landry and Kirchman, 2002).

Microzooplankton (whose root word "plankton" means "animal drifter" in Greek), and the smaller nano-zooplankton, most of which are protists, are the primary consumers of phytoplankton. Micro- and nano-zooplankton may be mixotrophic, feeding on other organisms as energy sources as well as making their own food via photoautotrophy (Stoecker, 1998). Although their name suggests they move about via drifting, they are also capable of locomotion. The designation "micro" in "microzooplankton" indicates a cell diameter of 20-200 micrometers. Copepod nauplii (such as *B. similis*), ciliates and dinoflagellates are main general groups of microzooplankton found commonly in our study area. Nanoplankton (2-20 micrometers) will also be included in this study, since they are the major grazers of picoplankton (0.2-2 micrometers), the smallest phytoplankton in the microbial food web and a very important component of the phytoplankton community in our study area. Our main focus, however, is on the grazing effect of microzooplankton.

1.2. Phytoplankton and algal blooms

Phytoplankton, whose name means "plant drifter" in Greek, is single-celled organisms which photosynthesize. They form the base of the oceanic food web. Many, if not most, phytoplankton are obligately photoautotrophic (they produce their own food via fixation of carbon dioxide using chlorophyll within the organism). Dinoflagellates can belong to different categories based on their feeding adaptation to their environment. Some species have the ability to either produce their own food (autotrophs) or consume other organisms (heterotrophs) based on the availability of food sources (mixotrophs), while others are strictly photoautotrophs or strictly heterotrophs. According to Sherr and

Sherr (2002), it is highly advantageous for a protist to be mixotrophic because it allows the protist to consume more of what they encounter. They do not have to be selective as to whether they are eating only autotrophs or only other heterotrophs; being able to consume both means the protist can reduce the clearance rate and thus its energy expenditure. For this study, we focused on the photoautotrophic phytoplankton. Cyanobacteria (*Prochlorococcus* and *Synechococcus*), diatoms and photoautotrophic dinoflagellates comprise the main types of phytoplankton identifiable in our samples and commonly found in nearshore environments. According to Partensky et al. (1999), high abundances of both PRO and SYN (*Prochlorococcus* and *Synechococcus*, respectively) in the mixed surface layer are a common distribution pattern nearshore.

Algal blooms are occurrences of intense and rapid growth of phytoplankton due to an excess of nutrients and escape from grazing control. Within phytoplankton populations, both diatoms and picophytoplankton will increase their abundance and biomass during favorable bloom conditions. At the beginning of a bloom, diatoms reproduce quickly, increasing their biomass by an order of magnitude. Initially, the diatoms increase at a rate that is faster than the grazers can control. The picoplankton show only a modest increase (Barber and Hiscock, 2006). While both diatoms and picoplankton increase during a bloom, so do grazers. The grazers eventually catch up to phytoplankton growth and regulate the picoplankton at a new, higher constant of biomass. During the course of the bloom, the diatoms, picoplankton and grazers keep each other in check: the diatoms compete among themselves for the most favorable space

and light conditions in which to increase their buoyancy and biomass; the picoplankton increase but are maintained at their new, higher constant by the grazers (Barber and Hiscock, 2006).

Storm runoff from streams into Kaneohe Bay provides one of the favorable conditions which may cause such phytoplankton blooms. The runoff contains large amounts of dissolved nutrients and particles which fuel an increase in primary productivity (DeCarlo et al., 2007). The biomass of these increases are often dominated by diatoms and dinoflagellates, and the dominance shifts temporally throughout the bloom (Hoover et al., 2006).

Phytoplankton are microscopic, single-cell organisms that thrive in tropical ocean systems while maintaining a rapid growth rate (Landry, 2002). Microzooplankton grazers serve as regulators for phytoplankton, keeping their populations relatively constant unless there is a disturbance in the balance, such as mixing or nutrient loading, as in storm runoff. For example, if grazers cannot consume the excess growth of phytoplankton after a storm, an algal bloom may occur. On the other hand, in absence of storms, mixing or nutrient loading, grazers may consume phytoplankton faster than they are able to grow, creating a decline in phytoplankton population. The regrowth of plant populations is determined by how efficiently the waste of grazers is remineralized as nutrients in the ocean, as well as how effectively phytoplankton compete with bacterial populations for mineral nutrients (Azam et al., 1983). In the biogeochemical cycle, these recycled nutrients are taken up as food by the phytoplankton.

1.3. Other factors affecting the microbial food web

Working with our growing understanding of the microbial food web, we must consider the dimension of interactions between autotrophic bacteria (*Prochlorococcus* and *Synechococcus* species, as found in our field samples) and heterotrophic flagellates, and how they provide the majority of the total energy transferred at the base of the food web. We must also consider how efficient the energy transfer is from primary producers (phytoplankton) to primary consumers (zooplankton). It has been determined that energy transfer rates at the microbial level are much higher than the top trophic levels. For example, there is a ~30% growth efficiency rate between phytoplankton and their primary consumers (the protist microzooplankton) (Straile, 1997), whereas the energy transfer rate among adult fish and top predators is significantly lower, at only 10% or less as the fish size increases because these top predators lose more energy to metabolism, as well as to reproductive and structural elements. (Mateo, 2007).

The amount of mixing from stream runoff after storms or from currents creates turbidity and clouds the water with sediments, reducing the depth that light penetrates the euphotic zone where phytoplankton grow. However, such mixing is also responsible for delivering nutrient loads to otherwise stratified and nutrient-deficient waters. According to Siegel et al. (2002), Sverdrup's 1953 critical depth hypothesis suggested a linear relationship between the amounts of available light and the depth of vertical mixing (Sverdrup, 1953). In waters with all needed nutrients, primary production could increase linearly depending on the amount of light penetrating the surface, and the depth to which it can penetrate the water column dictated the amount of primary production that could occur. Sverdrup's critical depth is defined as the depth where net production and net loss

(respiration) are equal. When a spring bloom begins, the mixed layer must be in shallow enough waters for light to penetrate the entire layer, and this layer must be above the critical depth. This means that production exceeds loss, and phytoplankton are able to increase their abundance, sometimes creating a bloom.

By that understanding, phytoplankton production would be at an annual low, without nutrient-loaded storm runoff, during the (storm-free) summer months; at that time, there is low disturbance, which leads to intense stratification and nutrient deficiency.

We will examine the meaning of chlorophyll levels in the discussion section but in general, we used flow cytometry and microscopic methods to try to determine the types and quantities of phytoplankton that had been selected by grazers. Phytoplankton abundance, as estimated by chlorophyll-a, for example, was shown to increase at sites that were near river mouths, as observed by Kamiyama (1994). Summer and autumn peaks of chlorophyll-a in the Seto Inland Sea in Japan indicated diatom blooms. Because phytoplankton contain chlorophyll, measuring the chlorophyll in a water sample can represent the presence and abundance of phytoplankton. In Hoover et al.'s 2006 studies of Kaneohe Bay, it was found that a gradual increase in chlorophyll-a levels corresponded with a shift in dominance during a bloom from smaller-cell phytoplankton to diatoms.

1.4. Grazing dynamics

1.4.1. General dynamics

The microbial food web is dominated by the smaller organisms, which are more efficient growers and grazers than their larger counterparts (Landry, 2002). Because

phytoplankton availability can change rapidly due to a variety of factors, the microzooplankton's fast growth rate helps them adapt equally quickly. This gives them a distinct advantage over the higher trophic levels such as metazoans, which are much slower to respond (Calbet and Landry, 2004).

In all regions of the world ocean, microzooplankton grazes at least 50% of the daily phytoplankton production, and in regions where <5 µm phytoplankton are dominant, grazers may consume fully 100% of daily phytoplankton growth (Sherr and Sherr, 1994). It has been observed that heterotrophic protists are able to grow faster than their phytoplankton food source because they can consume cells day and night, whereas phytoplankton can only build biomass during the day. It is by this dynamic that grazers are able to control the biomass and primary production of both heterotrophic and autotrophic microorganisms, even during the explosive phytoplankton growth exhibited by algal blooms (Sherr and Sherr 1988, 1994).

The successful replenishment and regrowth of phytoplankton populations is partly determined by the rate grazers are able to digest the nutrients from their phytoplankton prey. The waste products of micro-grazers are remineralized and the nutrients may be subsequently taken up by phytoplankton, closing the biogeochemical loop (Landry, 2002). Because of this recycling/remineralization process, it is the rapid feeding activity of micro-grazers that helps maintain the fast growth of the phytoplankton populations (particularly the smallest species) at a constant abundance. According to Irigoien's (2005) research of 12 different ocean regions, a general pattern was discerned: as phytoplankton biomass increased, microzooplankton biomass increased, but the microzooplankton biomass generally plateaued at around 50 µg C/L.

Another interaction we must consider with grazing dynamics is the effect the mesozooplankton (i.e., adult copepods) have on the microbial food web. Mesozooplankton prefer grazing on larger prey, such as other zooplankton (microzooplankton, such as ciliates and heterotrophic dinoflagellates) over phytoplankton. Referring back to **Figure 1**, this is the link between the microbial food web and the classic food chain mentioned earlier. This decreases the microzooplankton population, leaving fewer grazers to consume and control phytoplankton levels (Liu and Dagg, 2003, Sherr and Sherr, 2009). Mesozooplankton waste products also are involved in biogeochemical cycling, but since they package their waste (fecal pellets), the nutrients consumed tend to get removed from the upper water column in contrast to microzooplankton consumers.

1.4.2. In different ocean systems

Grazing dynamics varies based on ocean regions worldwide. For example, Liu and Dagg (2003) observed grazing dynamics in the Mississippi River plume in the Gulf of Mexico and found that phytoplankton growth was highest where the river entered the ocean and thus salinity was low, but microzooplankton growth rates were lowest at the same location, as shown by flow cytometry values. Liu and Dagg's experiments to obtain these results included Landry and Hassett's (1982) dilution techniques for showing phytoplankton growth rates and the rates of their micro-grazers. They also used the mesozooplankton addition approach (Calbet and Landry, 1999) to obtain measurements for mesozooplankton grazing rates. At a station further from the river mouth, phytoplankton growth remained high, but microzooplankton grazing rate was also

highest. Microzooplankton thrived in this area, far enough from the river mouth that sediments had begun to sink to the seafloor, yet still high enough in nutrients and with the clearest light to allow phytoplankton to grow abundant. All stations nearest the river mouth showed doubling rates of >1/day, with the nearest showing doubling rates of 2/day. At stations furthest from the river mouth, both phytoplankton growth and microzooplankton grazing rates decreased. This was due to nitrate limitations further out, since the majority of nutrients were quickly taken up nearest the river mouth. Other possible reasons of low growth and grazing levels could be aggregation (the clumping together of decaying phytoplankton) and their subsequent sinking out of the grazing zone at the surface.

This pattern suggests that we would only expect a similar situation to occur in Kaneohe Bay where a gradient of fresh and saline water occurs; that is, near enough to stream mouths to benefit from nutrient input from land, yet far enough that sediment has settled to the bottom and salinity was higher than the freshwater area of the river mouth, allowing a prosperous interaction of growth and grazing to take place. In Drupp et al. (2011), it was noted that the area of Southern Kaneohe Bay nearest the Kaneohe Stream input showed enhanced turbidity and lower salinity in the top 0.5 m layer. It was suggested that these less-than-optimal salinity and light conditions may reduce phytoplankton growth at that location, as opposed to areas further from the stream mouth, where salinity and light penetration were more suitable conditions for phytoplankton growth.

In areas like the Western Arctic Ocean, it was suggested by Sherr et al. (2009) that microzooplankton may have preferred heterotrophic flagellates over phytoplankton. Therefore, it appeared that microzooplankton grazing on phytoplankton was low.

In the Seto Inland Sea in Japan, chlorophyll-a indicative of diatom blooms occurred in summer and autumn, which in turn enhanced grazing (Kamiyama, 1994). The same pattern of distribution was found in this study as in the Mississippi River plume; that is, growth and grazing rates were highest nearer the river mouth, where chlorophyll-a was highest. It was also found that during algal blooms, certain phytoplankton were rejected for consumption by microzooplankton. The pattern showed that the microzooplankton population actually declined when the bloom was largest due to food rejection, and the microzooplankton population recovered once the bloom had decayed or otherwise dissipated. In the study described here for Kaneohe Bay, we looked at storm-influenced and non-storm influenced conditions, their resulting algal growth rates and how the microzooplankton responded with varying grazing rates.

1.5. Kaneohe Bay sampling site

We collected our water samples from the southern end of Kaneohe Bay, at 21°25’56.7”N, 157°46’47.1”W, in a smaller bay located southeast of Hawaii Institute for Marine Biology’s (HIMB) research island, Coconut Island. This particular, smaller bay was ideal due to surface mixing (mesotrophic waters), nutrient loading from the nearby streams and ample light penetration, all of which created a suitable environment for a phytoplankton bloom after a storm. Southern Kaneohe Bay is usually well-mixed in normal conditions. During storm conditions, stream runoff from the 3 main streams (see

Figure 2, below) add pulses of freshwater to the surface of the bay, and temporary stratified conditions are induced (Smith et al., 1981, Ringuet and Mackenzie, 2005).

Figure 2. DeCarlo's 2007 map (buoy markers removed) to show three input streams to South Kaneohe Bay: Keaahala, Kaneohe and Kawa.

1.6. Objectives of research and larger implications

In this experiment, we sought to determine the grazing rate of microzooplankton on phytoplankton and distinguish which groups of grazers play major roles in the food web dynamics of Kaneohe Bay. We found the microzooplankton (i.e., ciliates, dinoflagellates, copepod nauplii) consumed an average of 74% of daily growth in the week after a storm event, and an average of 154% of daily growth under non-storm influenced conditions. Quantifying the grazing impact of microzooplankton tells us how primary production cycles through the food web daily, and how much of that production is available to larger consumers.

Consequently, the amount of grazing at microbial levels influences success or failure of higher trophic levels, a valuable marine resource. Obtaining a more complete understanding of the microbial food web dynamics can influence management decisions regarding land-use planning, commercial and recreational uses of our coastal ecosystems.

2. METHODS

2.1. Field sampling methods

2.1.1. Field initial preparations

We conducted two sets of experiments in March 2012: Kaneohe Bay Grazing 1 (KBG1, on March 16-17, 2012) and 2 (KBG2, on March 30-31, 2012). The same collection methods, initial and final processing were conducted for both KBG1 and KBG2. All of the methods will be described in detail below for KBG1. KBG2 notes of differences in procedure, or of errors that occurred, will be at the end of each numbered methods section.

Our sampling site at starting position was 21°25.945 N, 157°46.785 W in the South Bay of Kaneohe Bay, near Coconut Island (See **Figure 3**, below).

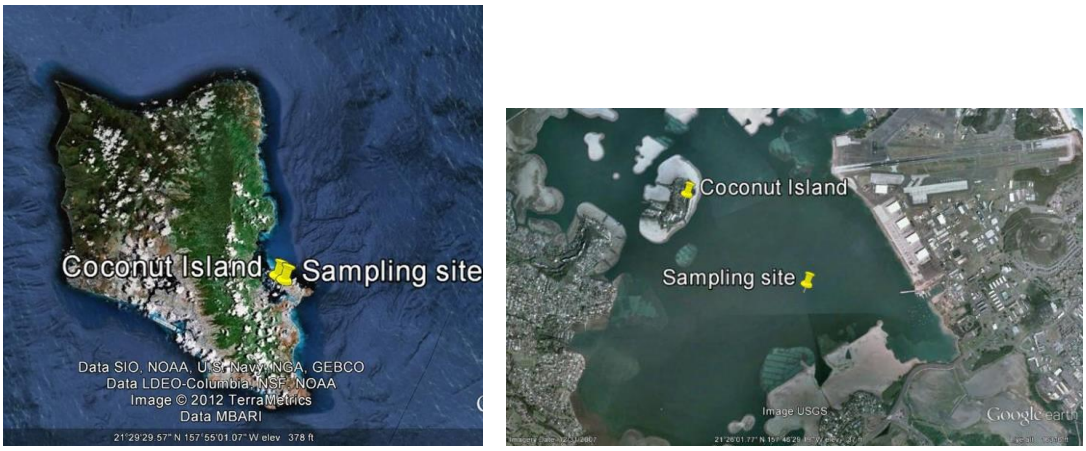

Figure 3. Maps of study site. A) The island of Oahu, with yellow pins at Coconut Island and sampling site. **B)** Close-up of Coconut Island and sampling site.

Five gallons of whole seawater were collected directly from the surface at a depth of less than 1 meter by filling a 5-gallon carboy over the side of the boat. A second collection at the same time of 5 gallons was also done. The second water sample was filtered through a 0.1-µm cartridge filter (Pall Acropak 500 Supor Membrane 0.1/0.1 µm, model #PN 1297) for use in the seawater dilution technique (Landry and Hassett, 1982).

The filtering process removed all cells. Adding varying percentages of filtered water to whole seawater allowed us to look at the net phytoplankton growth rate (gross growth rate – grazing-induced mortality rate) in the presence of varying impacts of microzooplankton grazers. This method relies on the assumptions that 1) the microzooplankton grazers are consuming cells at their maximum rate in the natural seawater, so that when the natural seawater is further diluted, the grazing rate is still maximum, and 2) diluting the seawater does not alter the gross growth rate of the phytoplankton cells, only the apparent net growth rate.

After returning to shore at Coconut Island, we rinsed 13 clear, plastic (polycarbonate) 1-liter bottles 3 times with freshly collected seawater. These bottles had been pre-soaked in 10% HCl. Once rinsed, bottles #1-10 were filled with the following dilution gradients of whole seawater to filtered seawater (WSW:FSW), at 2 bottles each: 1120 ml:0 ml; 920 ml:200 ml; 620 ml:520 ml; 420 ml:700 ml; 230 ml:890 ml. These bottles also had nutrients added: 1 ml each of $KH_4PO_4^-$ and NH_4Cl, for a final concentration of 10 µM $KH_4PO_4^-$ and 10 µM NH_4Cl. This was to ensure that there were plenty of nutrients available for phytoplankton growth in our incubation bottles, so that the gross growth rates measured would be maximal. This is necessary since dilution of the natural seawater and enclosure of that water in a bottle for our incubations would potentially disrupt the natural replenishment of nutrients through mixing and grazing remineralization processes. Two of the 13 1-liter bottles were used as control bottles to determine the phytoplankton gross growth rate with no nutrients added (100% seawater), as well as 1 bottle for a filtered seawater (0.1 µm) control.

The 13 clear, 1-liter bottles were capped and gently mixed by turning the bottles hand over hand, then 1.5 ml of water was removed from each bottle for an initial flow cytometry sample (1.5 ml sample + 75 µl 10% paraformaldehyde). The experimental bottles were then tightly capped and placed in a clear, Lucite box with large perforations to allow water to flow through it. This incubator was anchored to the seafloor of the marina on the bank, at a 1 m depth from the surface, to simulate the light conditions of the surface water site from which we collected the original samples. The incubator was left in place for 23 hours.

Other initial samples were taken from the seawater carboys as follows: the details of processing these samples are described below. Two separate, opaque, 250 ml bottles were filled with whole seawater for chlorophyll-a measurements later in the lab. These samples were kept in the dark on blue ice until processed in the laboratory. One 500 ml dark bottle and one 50 ml tube were filled and preserved with 20 ml and 2 ml, respectively, of 10% paraformaldehyde on site for later use in preparation of epifluorescent microscopy slides. One 250 ml dark bottle was filled with seawater and preserved with 20 ml of Acid Lugols solution (~1% final concentration, Throndsen 1978) for use in a settled slide sample (for counting ciliates) later in the lab.

2.1.2. Field final preparations

After ~24 h of in situ incubation, the experimental bottles were removed from the incubator and taken ashore for processing. As outlined for the initials above, we preserved samples for the epifluorescent slides, the Acid Lugols slides and the flow cytometry analyses immediately at the site. We also filled 13 dark 250 ml bottles from

each of the incubated samples; these 250 ml samples were filtered within 3 hours at the lab for chlorophyll determinations and are described below, in lab sampling methods.

Flow cytometry samples and small volume epifluorescent slide samples were taken from all 13 bottles, whereas acid Lugols samples and large volume epifluorescent slide samples were taken from the most dilute treatment bottle and two of the whole seawater bottles (bottles 1, 10, and 12).

2.2. Laboratory sampling methods:

2.2.1. Flow cytometry

Flow cytometry was used to determine the abundance of phytoplankton and bacteria cells in each 1.5 ml aliquot water sample. These samples were preserved on site (as outlined above), then frozen to -80°C until run in batches on the flow cytometer. For processing, the samples were stained with Hoechst dye (DNA stain) for 1 hour (final dye concentration 1 µg/ml). The stained samples were analyzed using a Beckman-Coulter Altra flow cytometer mated to an Orion syringe pump, using dual laser excitation (UV and 488 nm) to gather the fluorescence signatures of chlorophyll, phycoerythrin, and DNA, as well as forward and 90° light scatter. Subsequently, the data were analyzed in FlowJo software to obtain the abundance of cells. Populations distinguishable by this method are *Prochlorococcus* spp., *Synechococcus* spp., photosynthetic eukaryotes, and non-pigmented bacteria.

2.2.2. Chlorophyll

2.2.2.1. Sample preparation

For preparation of chlorophyll samples in the lab, we poured the replicate bottles of 250 ml chlorophyll samples (duplicate for KBG1 and triplicate for KBG2) through

separate funnels on a vacuum filtering system onto GF/F filters. These samples were then wrapped in foil and stored at -80°C until processed later in a batch. The finals samples for both experiments were treated the same way ~24 hours later.

2.2.2.2. Chlorophyll sample processing

When ready to process, the chlorophyll filters were thawed in batches, 5 ml of 90% acetone was added to each, and then the chlorophyll was extracted by freezing at -80°C for 24 hours. Subsequently, the extracted samples were processed through a fluorometer (Turner 111 with F4T5 lamp and red-sensitive photomultiplier). Each sample was read on the fluorometer before and after acidification, to determine the amount of chlorophyll-a and phaeopigment present. The pigments are extracted in acetone and they will fluoresce in a fluorometer in proportion to the amount chlorophyll present in the sample. After acidification, all of the chlorophyll in the samples is converted to its degradation product, phaeopigment, and the fluorescence from that is also measured.

For the fluorometry procedure, we placed a sample vial in the compartment and took a "reading before" (Rb) measurement. We then added 2 drops of 5% HCl, and using our thumb (instead of capping sample) we inverted sample 3 times to mix and acidify the sample. We placed the sample back into the fluorometer and took a "reading after" (Ra) measurement. We recorded our measurements into a spreadsheet. We blanked the fluorometer after every 2 samples, using the blank. All of our initial samples were whole seawater. For KBG1, we processed 2 initial samples and 13 final samples. For KBG2, we processed 3 initial samples and 13 final samples. Sample 13 was the 0.1 µm-filtered seawater sample, which we used as a blank.

2.3. Slide preparation

2.3.1. Epifluorescent slides

2.3.1.1. Initials

Upon returning to the UH campus from the field from setting up the experimental incubation, we prepared epifluorescent microscopy samples by staining them with a protein dye (proflavin) and a DNA dye (DAPI). The correct procedure was to add 50 µl 0.2-µm sterile filtered proflavin (full name: Proflavin, 3,6-diaminoacridine, hemisulfate salt; final concentration 0.033%) to the 50 ml (small volume) tube and 200 µl to the 500 ml bottle and stain them both for 30 minutes in the dark.

Then, the samples were filtered onto black polycarbonate filters: for the 50 ml sample, the pore size was 0.8 µm and for the 280 ml sample it was 8 µm. When ~10 ml of sample remained in the filter tower, the fluorescent dye DAPI (4',6-diamidino-2-phenylindole) was added (final concentration 1 µg/ml). DNA staining lasted 3 minutes, then the sample was filtered to dryness. We mounted the filters on glass slides using immersion oil. We placed the filters onto one spread drop of oil using forceps, then put another drop of oil on top of the filter and placed a glass slide cover on top of the filter. We did this for all initial and final slides. All slides were stored in a slide case and frozen at -80°C until later processing for epifluorescence microscopy.

In KBG1, we initially used the wrong size black polycarbonate pore size filters for our initial samples. We used an 8-um pore size filter for the initial small volume (50 ml sample), and 0.8-um pore size filter for the 280 ml large volume initial sample. Therefore, we made two additional preparations using the correct sizes of filters per

volume of samples: one using an additional 50 ml of sample onto a 0.8-µm pore size filter, and one using the remaining samples (280 ml) onto a 8-µm pore size filter. All 4 samples were frozen for later processing.

2.3.1.2. Finals

After returning from the field to take down the experimental incubations, ~24 hours after set up, we prepared epifluorescent microscopy slides from 3 large volume 500 ml samples from experimental bottles 1, 10 and 12; and 13 small volume 50 ml samples from each of the 13 bottles. We added 400 µl of proflavin to the 500 ml bottles; we added 100 µl of proflavin to the 13 small volume bottles. We allowed this solution to stain for 30 minutes in the dark. The samples were filtered onto 0.8 or 8 µm filters (as appropriate for the sample type, as outlined in the previous section) until about 10 ml were left in the filter towers, then we added approximately 1 ml portions of DAPI to all samples and allowed solution to stain a further 5 minutes, before finishing the filtration. We mounted the filters on glass slides as outlined previously. All slides were stored in a slide case and frozen at -80°C until further processing.

We made the following errors and notes for the final samples: for the small volume slide preparations, sample 1 had unfiltered DAPI added to it. Sample 4 had DAPI added to a dry filter. We spilled sample 11 and so this sample was lost. For the large volume slides: sample 10 had an Appendicularian on the filter; we removed the organism prior to freezing the slide.

2.4. Microscope processing

2.4.1. Epifluorescent scope

Digital photos of the slides we prepared for KBG1 and KBG2 were taken. To do this, we thawed the frozen slides for 1 minute at room temperature, then blotted away the condensation moisture. We thawed only 1-2 slides right before we photographed them in order to preserve the fluorescence integrity of the samples.

To image the slides, we used the software program Microfire, attached to an epifluorescent microscope (Olympus Model BX51 TRF), camera (Olympus U-LH100HGAPO) and computer. For the large volume slides, the magnification was 10x (ocular) x 20x (objective) for a total magnification of 200X; for the small volume slides, the objective used was 40x, for a total magnification of 400X. For each slide, we moved the stage to 30 random locations; at each location, we took 3 micrograph images using 3 different excitation/emission filters. Filter 1 showed chlorophyll (excitation = 450-480 nm, DM = 500 nm, emission = 515 nm); filter 2 showed mainly *Synechococcus* (excitation = 520-550 nm, DM = 565 nm, emission = 580 nm); filter 3 showed DNA excited by UV fluorescence (excitation = 330-385 nm, DM = 400 nm, emission = 420 nm). Images were saved as jpg files for subsequent analyses and the microscope slides were re-frozen after imaging for archival purposes.

For the next step, we analyzed the contents of each of the 30 images per slide for the large volume initial slides for KBG1 and KBG2. We used Zeiss software (Zeiss Image, version 3.0.00.00) to count and size every organism that was >2 um in length and >2um in width. We created an Excel spreadsheet depicting the object's number, length, width, whether it was a heterotroph or autotroph, and notes to help identify and describe the various organisms counted.

2.5. Spreadsheet processing and calculations

We used the following spreadsheet data for the next step in processing the data from the imaged initial large volume slides.

In Excel, we created a separate spreadsheet for each of the above slides. We added a column for volume (um^3) and used the formula for a prolate spheroid:

$$\text{Biovolume} = 4/3 \times 3.14 \times (\text{width}/2)^2 \times (\text{length}/2)$$

This formula was applied to every counted object. Next, we sorted all objects by heterotroph or autotroph. Then, we sorted the autotrophs by whether they were diatoms or non-diatoms. We then sorted objects within their autotroph or heterotroph groups by their cell length into the following categories: 2-5 um, 5.1-10 um, 10.1-20 um and >20.1 um.

The biovolumes were converted into biomass using the following equations from Menden-Deuer and Lessard (2000):

- For diatoms: pg C/cell = $0.288 \times (\text{Volume})^{0.811}$
- For non-diatoms (other heterotrophs and autotrophs): pg C/cell = $0.216 \times (\text{Volume})^{0.939}$

Next, we summed the cells in each size category of biomass (pg C/cell) to calculate the biomass in each field imaged on each slide (pg C/field), the number of fields per slide, the area of the slide, and the volume filtered for each slide to calculate the biomass of plankton (ug C/Liter) in each sample:

Biomass (ug C/L) = (pg C/field) x (field/area) x (area/slide) x (slide/volume filtered in ml) x (1000 ml/L) x ($ug/10^6 pg$).

Next, we calculated the abundance (cells/ml) for each size category in an analogous fashion, using the following equation:

Abundance (cells/ml) = (cells/field) x (field/area) x (area/slide) x (slide/volume filtered in ml).

For the next part of the calculations, we took the data above (biomass or abundance for each field, ~30 fields/slide, 2 separate slides) and put them into a new spreadsheet. Within each slide image, we grouped remaining objects by diatom, autotroph or heterotroph and within each of those, by the size categories listed above. We summed only the biomass and abundance, then put only those sums into another spreadsheet.

Next, we took all the sums for biomass and abundance and grouped them all according to size categories, discarding the individual object numbers and field numbers. For example, for each slide, we obtained a set of sums for each size category of diatoms, autotrophs and heterotrophs.

We then condensed this into a small table on another spreadsheet. We calculated the average and standard deviation for each size category, for both biomass and abundance. We summed the categories to reach one final total for all autotrophs (including diatoms) and for all heterotrophs.

2.5.1. Biomass and abundance table

We transferred the microscope data into a spreadsheet called Biomass and Abundance, which showed data for both the KBG1 and KBG2 slides. We added our flow cytometry data for biomass and abundance for the categories *Prochlorococcus* (PRO), *Synechococcus* (SYN), Photosynthetic eukaryotes (PEUK), Heterotrophic bacteria (HBACT) on this table. We used the following conversion factors to change our flow cytometry abundance data (cells/ml) to biomass (µg C/L):

- For PRO (Shalapyonok, et al., 2011): 3.3×10^{-8} µg/PRO cell
- For SYN (Garrison et al., 2000): 1.02×10^{-7} µg/SYN cell
- For PEUK (Eppley et al. 1970: $\log_{10}C=0.94*\log_{10}BV - 0.60$, where BV (biovolume) was estimated from the average biovolume calculated using epifluorescent microscopy for the 2-20 µm diameter cells)
    - KBG1: 96×10^{-6} µg/ PEUK cell
    - KBG2: 70×10^{-6} µg/PEUK cell
- For HBACT (Christian and Karl, 1994): 1×10^{-6} µg/HBACT cell

2.5.2. Growth and grazing rates table to FCM graphs

We compiled data from KBG1 and KBG2 for bottles 1-12 to create a table of Growth and Grazing Rates. The table includes data from KBG1 FCM, KBG2 FCM and chlorophyll data. The growth and grazing table contained data for the 4 flow cytometry populations: PRO, SYN, PEUK, and HBACT. The data for each of the 4 categories was: abundance (initial and final cells/ml); dilution factor (percent of whole seawater: filtered seawater) and net phytoplankton growth per day.

A sample table of PRO data is shown below in **Table 1**. The complete data for all categories of KBG1 and KBG2 can be found in **Table A1**, **Appendix A**.

Table 1. KBG1 Abundance data from flow cytometry, as well as calculated dilution factors and net growth rates (k, d^{-1}).

Prochlorococcus				
Incubation bottle No.	**cells/ml (initial)**	**cells/ml (final)**	**Dilution Factor**	**k (d^{-1})**
1	36142	118590	0.17	1.19
2	41581	111470	0.20	0.99
3	77816	90123	0.37	0.15
4	78266	178196	0.37	0.82
5	115784	238569	0.55	0.72
6	118219	236346	0.56	0.69
7	168416	288236	0.80	0.54
8	170374	280931	0.81	0.50
9	208925	255231	1.00	0.20
10	208422	201196	1.00	-0.04
11	209137	250374	1.00	0.18
12	214272	343978	1.00	0.47

The dilution factor for each sample incubation bottle was calculated by taking the ratio of the initial abundance to the average of the 100% initial abundance for each dilution bottle. For example, the average initial *Prochlorococcus* abundance in the whole seawater (100%) bottles (bottle numbers 9-12) is 210,189 PRO cells/ml, and the initial PRO sample 1 abundance is 36,142 cells/ml. Thus, the dilution factor is calculated as 36,142/210,189 = 0.17. The net growth of phytoplankton (k, d^{-1}) was calculated assuming exponential growth, as follows:

Net growth rate (k, d^{-1}) = LN((Abundance-final)/(Abundance-initial))/t,

where t = 1 day (incubation time).

Note that no flow cytometry data were obtainable for KBG2 Sample 9, likely because the sample tube had large particles in it (dirt) when the sample was taken, making it un-analyzable.

We plotted FCM graphs for KBG1 and KBG2, for each of the four flow cytometry categories; therefore, we made 8 graphs from this data. We plotted the dilution factor versus net growth per day for incubation bottles 1-12. Bottles 1-10 were the incubation bottles with nutrients added. For each graph, we plotted bottles 11-12 separately, since they were the no nutrient-added control bottles.

We used Excel to perform a linear regression analysis on each graph for bottles 1-10 only. The coefficient of determination, r^2, was used to show how much of the variability in the data is explained by the regression line. We made a separate average calculation for bottles 11-12 to estimate the net growth rate of the phytoplankton cells without added nutrients.

The linear regression line, $y = mx + b$ given by the regression analysis represents the following variables: m = the slope = the mortality rate due to grazing; $u_n = b$ = the y-intercept of the line = the gross growth rate of the phytoplankton with nutrients added. μ_0 was obtained from the sum of the mortality rate (m) and the average net growth rate calculated for bottles 11-12 (k_0, no nutrients added). In other words: $y = mx + b$ = (mortality rate)x (dilution factor) $+ u_n$ and $\mu_0 = k_0 + m$.

2.5.3. Regression table

We compiled the data for PRO, SYN, PEUK and HBACT from KBG1 and KBG2 into one final table, which showed the totals for u_0 (growth rate without nutrients); for u_n

(growth rate with added nutrients); and for mortality (grazing rate from the slope in the line equation). The μ_0 (gross growth rate of phytoplankton without nutrients added) was calculated as $\mu_0 = (k_0 - m)$.

3. RESULTS

3.1. Study site

KBG1 was our storm-influenced experiment because a rainstorm occurred less than 5 days prior to our collection date (See **Table 2A**, below). Note that this storm-influenced period began several days earlier (March 4), with thunderstorms and rainshowers lasting several days, and included reports of hail in Kaneohe Bay (*www.youtube.com/watch?v=ATZXrJSr6Ew)* and sewage outfall overflows (http://www.hawaiinewsnow.com/story/17086379/rain-causes-sewage-spill-into-kaneohe-bay). KBG2 was our non-storm experiment because there were no rainstorms within 5 days of our collection date (See **Table 2B**, below). A graphical representation of precipitation can be viewed below in **Figure 4**.

Table 2. Daily Precipitation totals for KBG1 (A, left) and KBG2 (B, right) for 11 days prior to and including collection date. Abbreviations in table are as follows: TSRA = thunderstorm with rain, RA = rain, BR = mist, VCTS = thunderstorm in vicinity, SHRA = rain shower. Data courtesy of NOAA National Climatic Data Center's Quality Controlled Local Climatological Data.

A. KBG1 (storm): March 6-16, 2012		
Date	**Precipitation (mm)**	**Comment**
3.06	39.37	TSRA RA BR VCTS
3.07	4.83	SHRA
3.08	15.49	RA
3.09	2.03	RA BR
3.10	1.02	SHRA
3.11	2.29	RA BR
3.12	0.25	
3.13	0.25	RA SHRA
3.14	0.25	
3.15	1.78	RA
3.16	0.25	RA
total	**67.81**	

B. KBG2 (non-storm): March 20-30, 2012		
Date	**Precipitation (mm)**	**Comment**
3.20	0.00	
3.21	1.78	RA SHRA
3.22	1.52	RA
3.23	2.03	RA
3.24	2.29	RA SHRA
3.25	1.2	RA
3.26	trace	
3.27	2.79	RA
3.28	0.00	
3.29	trace	RA
3.30	0.00	
total	**11.61**	

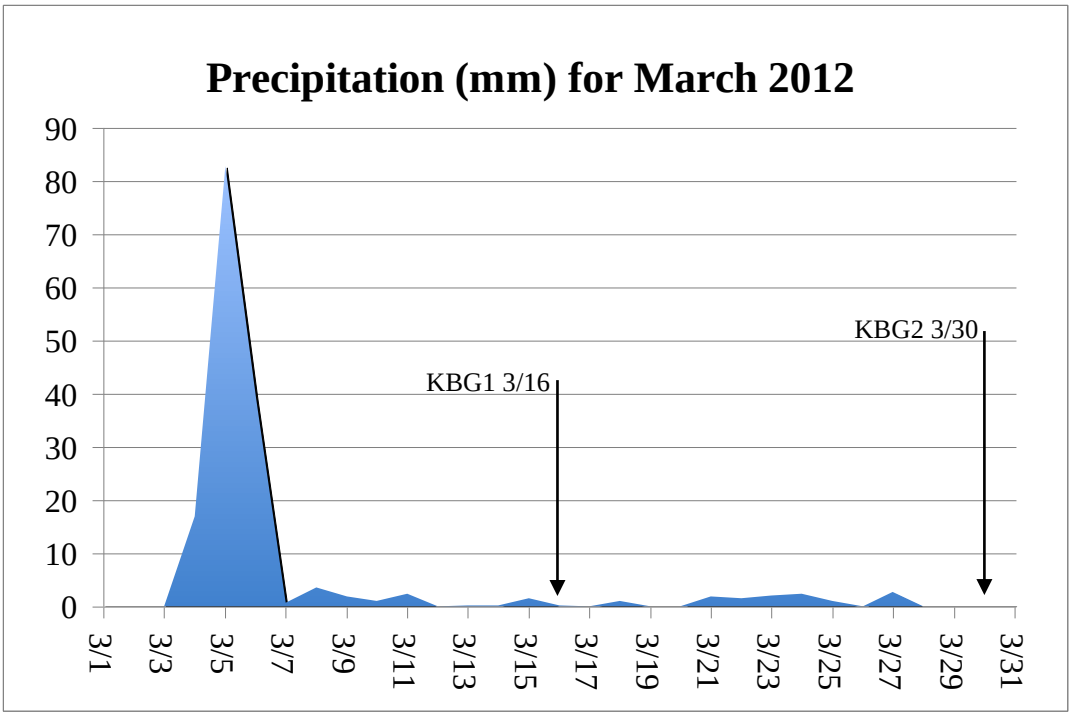

Figure 4. Precipitation data for March 2012, Kaneohe Bay. Sampling dates marked with arrows.

3.2. Biomass and abundance

3.2.1. KBG1 biomass and abundance data

The data described in this section are listed in tabular form in **Table 3**. They are derived from analyses of the epifluorescent microscopy and flow cytometry data from the initial samples from each experiment, and thus represent the state of the microbial community as sampled from Kaneohe Bay, prior to the experimental incubation.

Table 3. Microbial biomass and abundance data from experiments KBG1 and KBG2 conducted in Kaneohe Bay. Autotrophs (a) and heterotrophs (h) as measured using epifluorescence microscopy are arranged by length size classes (µm), with diatoms indicated separately. Also included are the flow cytometrically-derived populations Prochlorococcus (PRO), Synechococcus (SYN), Heterotrophic bacteria (HBACT), and photosynthetic eukaryotes (PEUK).

	KBG1		KBG2	
Category	**Biomass (µg C/L)**	**Abundance (cells/ml)**	**Biomass (µg C/L)**	**Abundance (cells/ml)**
AUTOTROPH EPIFLUORESCENT MICROSCOPY DATA				
a 2-5 µm	0.08 ± 0.07	23 ± 20	0.13 ± 0.08	40 ± 23
a 5.1-10 µm	1.06 ± 0.81	47 ± 32	1.26 ± 0.46	58 ± 24
a 10.1-20 µm	6.61 ± 3.96	67 ± 35	4.40 ± 2.04	45 ± 22
a 20.1+ µm	43.58 ± 81.20	23 ± 20	34.17 ± 50.20	29 ± 39
diatoms	8.74 ± 15.84	133 ± 94	0.24 ± 0.42	6 ± 9
AUTOTROPH FLOW CYTOMETRY DATA				
PRO	0.01 ± 0.0001	$2.1 \pm 0.03 \times 10^{5}$	0.01 ± 0.0006	$2.4 \pm 0.2 \times 10^{5}$
SYN	0.02 ± 0.0001	$1.7 \pm 0.07 \times 10^{5}$	0.03 ± 0.002	$2.6 \pm 0.1 \times 10^{5}$
PEUK	2.7 ± 1.1	$2.8 \pm 0.3 \times 10^{4}$	0.8 ± 0.13	$1.2 \pm 0.21 \times 10^{4}$
HETEROTROPH EPIFLUORESCENT MICROSCOPY DATA				
h 2-5 µm	$0.2 \pm 0.9 \times 10^{-2}$	1.0 ± 4.0	none	none
h 5.1-10 µm	0.11 ± 0.25	4.0 ± 7.0	0.01 ± 0.03	1.0 ± 2.0
h 10.1-20 µm	1.28 ± 1.70	8.0 ± 11.0	0.16 ± 0.43	1.0 ±4.0
h 20.1+ µm	270 ± 690	12 ± 13	5.41 ± 29.23	0.4 ± 1.0
HETEROTROPH FLOW CYTOMETRY DATA				
HBACT	$1.4 \pm 0.1 \times 10^{-2}$	$1.43 \pm 0.9 \times 10^{6}$	$1.5 \pm 0.1 \times 10^{-2}$	$1.50 \pm 0.07 \times 10^{6}$

3.2.1.1. Epifluorescent microscopy data

The phytoplankton and heterotrophic grazers found on the microscopy slides were divided into size classes (**Table 3**). With the exception of the diatoms, there is little pronounced difference between the experiments in terms of biomass or abundance between KBG1 and KBG2 sampling dates. The epifluorescent microscopy slides showed that the highest biomass for the autotrophs was found in the >20.1 µm size category, at 43.58 ± 81.20 µg C/L in KBG1 and 34.17 ± 50.20 µg C/L in KBG2. The highest biomass for heterotrophs was also found in the >20.1 µm size category: 270 ± 690 µg C/L for KBG1 and 5.41 ± 29.3 µg C/L for KBG2. The biomass due to diatoms was 8.74 ± 15.84 µg C/L in KBG1, relative to only 0.24 ± 0.42 µg C/L in KBG2. The 10.1-20 µm diameter autotrophs continue this trend of higher values for biomass in KBG1 versus KBG2, with 6.61 ± 3.96 µg C/L and 4.40 ± 2.04 µg C/L, respectively. Similarly, the 10.1-20 µm heterotrophs also have more biomass during KBG1 vs. KBG2 (1.28 ± 1.70 µg C/L vs. 0.16 ± 0.43 µg C/L, respectively). Note the large variance on these biomass estimates, which is due to the imprecision of the microscopy method, especially for these larger, relatively rare cells. For the smaller cells, there was little difference in biomass between the two experiments, although, unlike the trend for the larger cells, KBG2 had slightly higher biomass and abundance values in the 2-5 µm and 5-10 µm categories relative to KBG1. Abundance trends generally followed those just described for biomass, with larger autotroph and heterotroph cells most abundant in KBG1 and the smallest (<10 µm) autotrophs more abundant in KBG2.

3.2.1.2. Flow cytometry data

The flow cytometry data showed the presence of ~10^5 cells/ml of the pico-phytoplankton *Prochlorococcus* (PRO) and *Synechococcus* (SYN) on both sampling days.) Non-pigmented bacteria (or heterotrophic bacteria, HBACT) were also found at a concentration of ~1.4-1.5 x 10^6 cells/ml on the two sampling days.

The lowest biomass for autotrophs was *Prochlorococcus,* in the <2 µm size category, at 0.01 ± 0.0001 µg C/L in both experiments, although this group was usually the most abundant (~2 x 10^5 cells/ml). In terms of trends between experiments, there were more PRO than SYN in KBG1, whereas in KBG2 there were slightly more SYN than PRO. The photosynthetic eukaryotes (PEUK) had an abundance and biomass in KBG1, of 2.8 ± 0.3 x 10^4 cells/ml and 2.7 ± 1.1 µg C/L, respectively. This was much higher than the PEUK abundance and biomass found for KBG2, of 1.2 ± 0.21 x 10^4 cells/ml and 0.8 ± 0.13 µg C/L, respectively.

3.2.2.3. Qualitative comparisons for Tables 3 and 4.

For diatoms, both biomass and abundance were higher in KBG1 than in KBG2. Here we include some representative microscope photos **(Figures 5-7, below)** that illustrate the differences in abundance and species composition between the two experiments. **Figures 5A and 6A** micrographs were taken using the chlorophyll filter previously detailed in the Methods section. **Figure 5A** is representative of typical composition of KBG1 storm conditions, while **Figure 6A** represents the composition of KBG2, non-storm conditions. In these images, red color denotes chlorophyll and green color is from proteins. The background is the black membrane filter, with the pores in the membrane visible as circular objects in the image. High diatom abundance,

specifically chain-forming centric *Chaetoceros sp.*, dominated. The chains pictured were in the expected >20.1 µm size category, and measured 128 µm.

Figures 5B and 6B micrographs were taken using a UV filter, also detailed in the Methods section. The bright, white-bluish dots represent DAPI-stained nuclear DNA. **Figure 5B** shows a composition typical of KBG1, the storm conditions, while **Figure 6B** shows KBG2, the non-storm conditions. Low to no diatoms were present. High abundance of smaller cells (0.2-2 µm), specifically the picoplankton *Synechococcus*, dominated. Our composition findings for storm and non-storm conditions agreed with the prior research findings of Hoover et al. (2006), where smaller, more nutrient-efficient cells dominated the nutrient-stressed non-storm conditions; and where the larger cells (diatoms) thrived with the plentiful nutrient input from storm conditions. **Figures 7A** (chlorophyll filter) and **7B** (UV filter) micrographs, below, depict a pennate diatom from KBG1 storm conditions and are of characteristic size, at 73 µm.

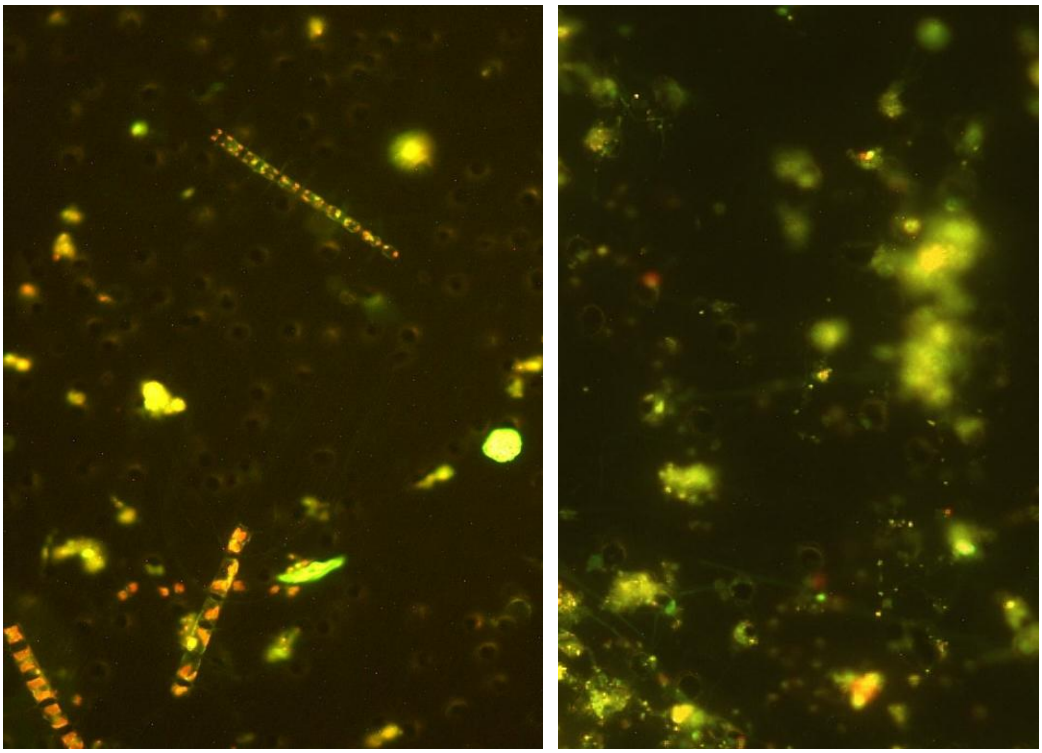

Figure 5A (left) and Figure 6A (right). Typical biomass compositions for KBG1 storm (left) and KBG2 non-storm (right). Magnification 200x. Chlorophyll filter.

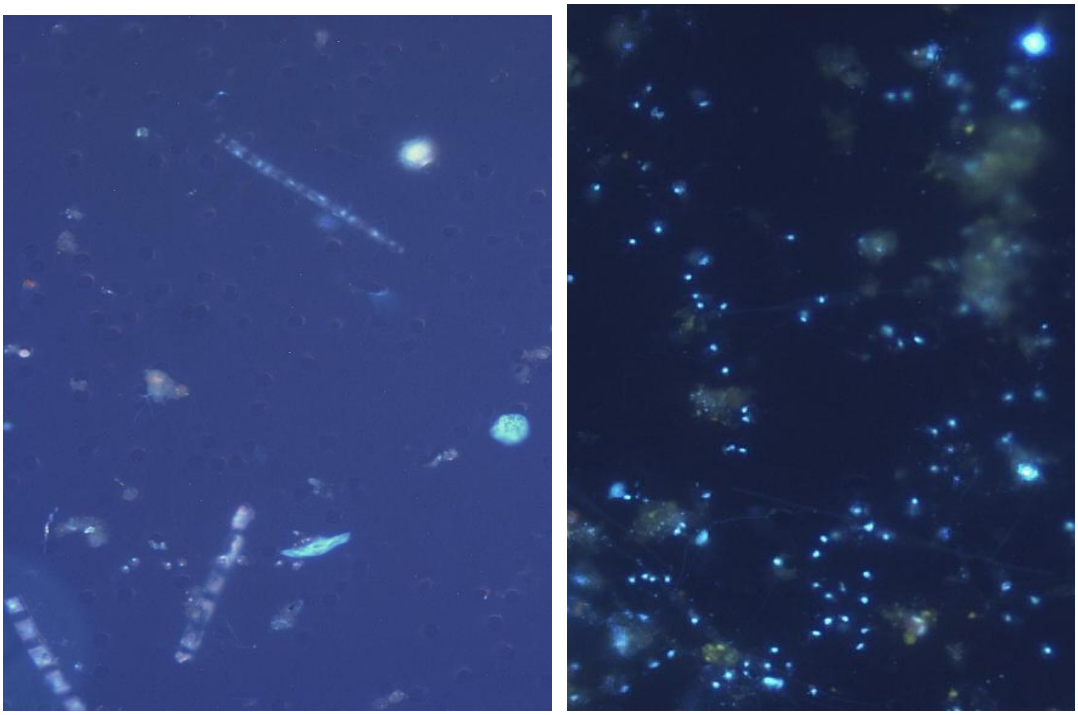

Figure 5B (left) and Figure 6B (right). Typical biomass compositions for KBG1 storm (left) and KBG2 non-storm (right). Magnification 200x. UV filter.

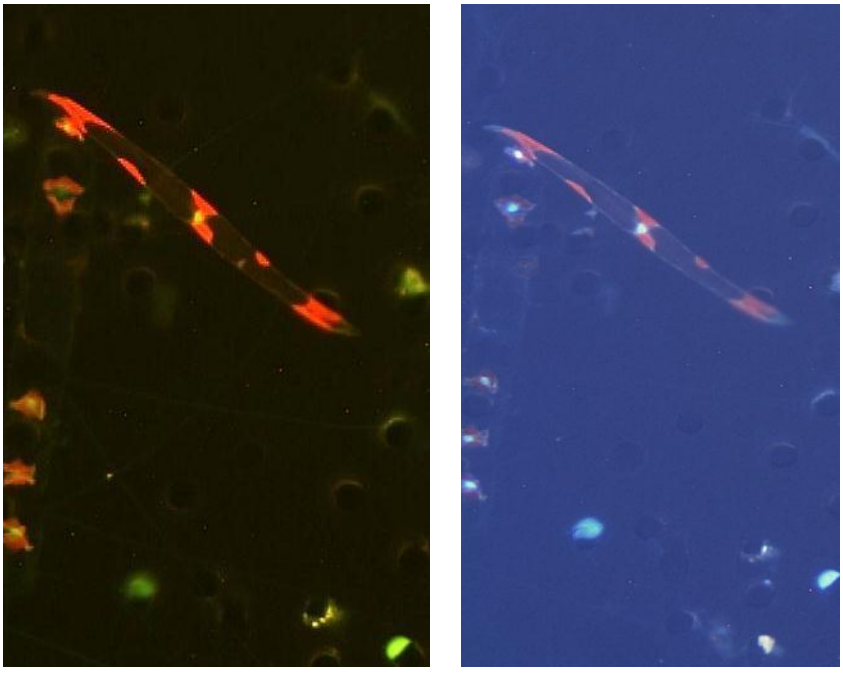

Figures 7A (left) and 7B (right). Pennate diatom, KBG1. Magnification 200x. Chlorophyll filter (left) and UV filter (right).

3.3. Flow cytometry graphs and rates of growth and grazing

For complete data for the pico- and nano-plankton (PRO, SYN, PEUK, HBACT) abundance and rate estimates from flow cytometry samples taken during KBG1 and KBG2 experiments, please refer to **Table A1 in Appendix A**.

One sample in KBG2, from bottle 9, had large particles in it and so was not analyzable by flow cytometry.

3.3.1. Net phytoplankton growth (k d^{-1}) compared between KBG1 and KBG2

The FCM graphs depicted in **Figures 5 and 6** (below) show the results from the KBG1 and KBG2 experiments for the analyses of the flow cytometry samples for the following populations: *Prochlorococcus, Synechococcus*, photosynthetic eukaryotes and heterotrophic bacteria. We plotted the dilution factor (% whole seawater) versus the net growth rate (units: per day) of phytoplankton. The dilution factor represents how much

the incubated sample was diluted with filtered seawater, resulting in a decrease in grazing pressure at higher dilution factors. Numerical data correlating to the FCM graphical results are presented in **Table 4**, following FCM graphs, (below).

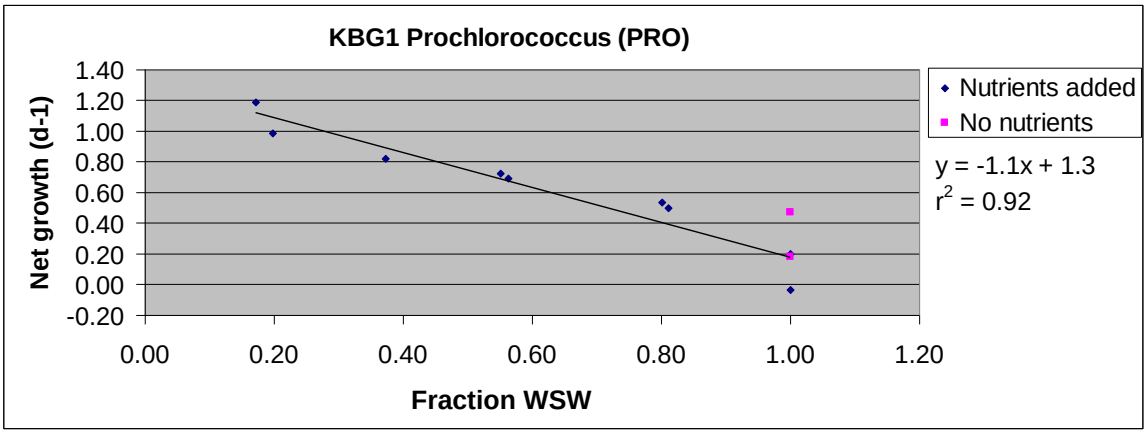

Figure 8A. KBG1 PRO FCM, dilution factor vs. net growth per day.

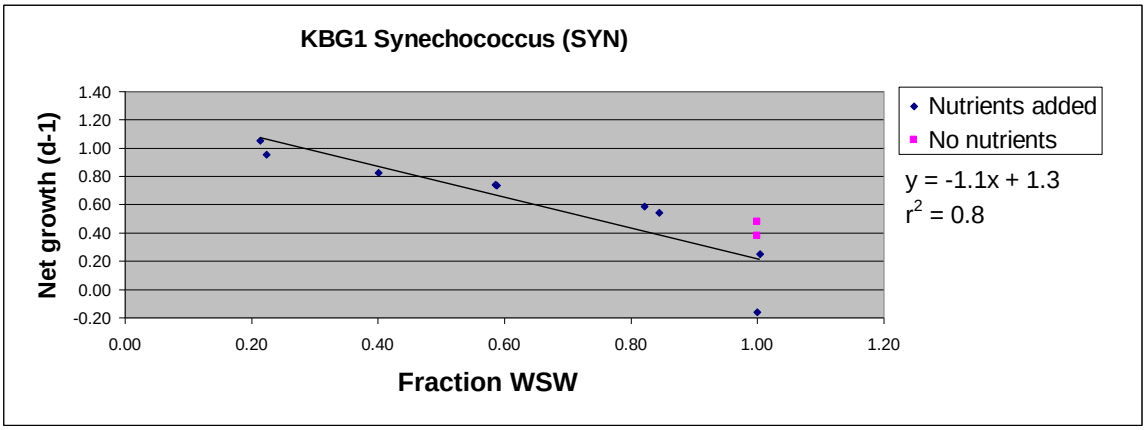

Figure 8B. KBG1 SYN FCM, dilution factor vs. net growth per day.

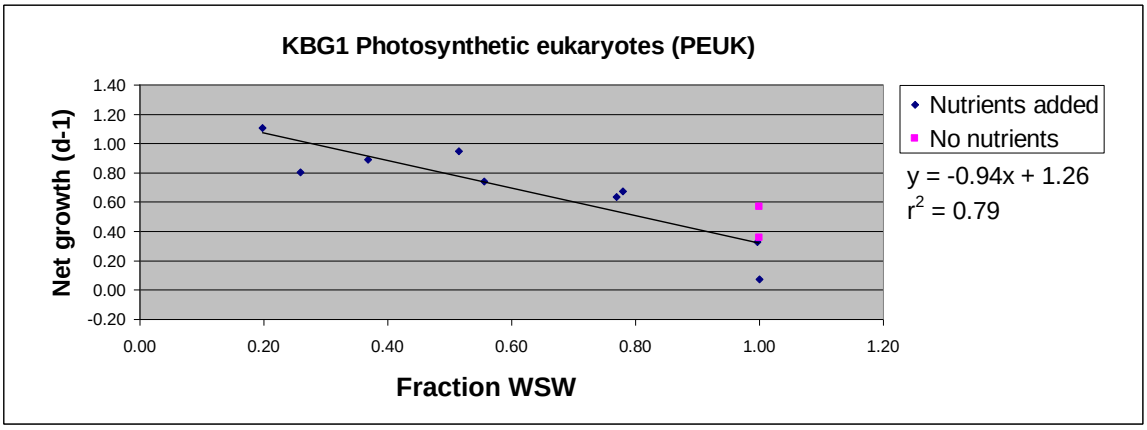

Figure 8C. KBG1 PEUK FCM, dilution factor vs. net growth per day.

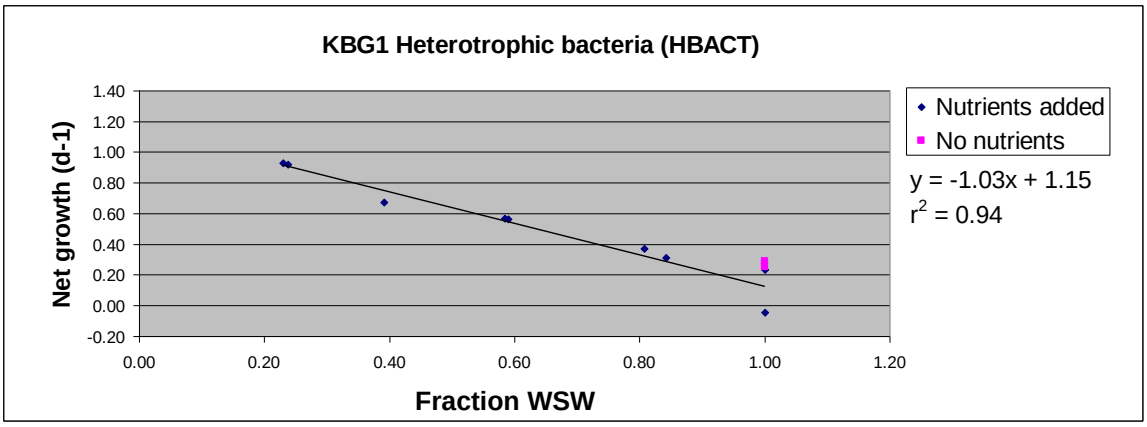

Figure 8D. KBG1 HBACT FCM, dilution factor vs. net growth per day.

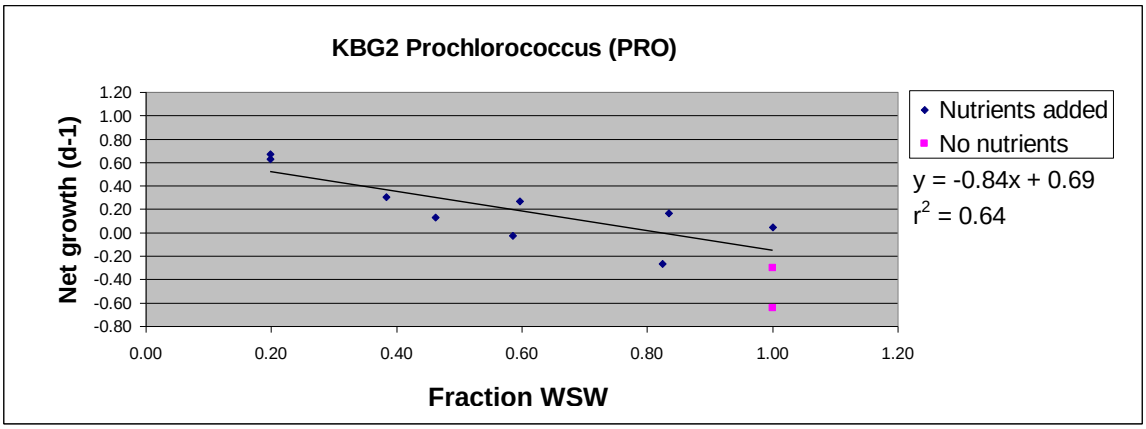

Figure 9A. KBG2 PRO FCM, dilution factor vs. net growth per day.

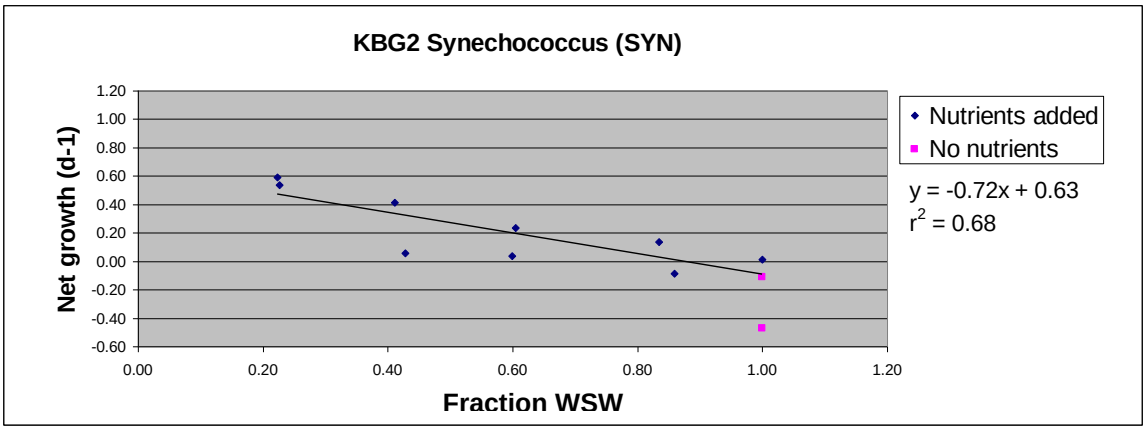

Figure 9B. KBG2 SYN FCM, dilution factor vs. net growth per day.

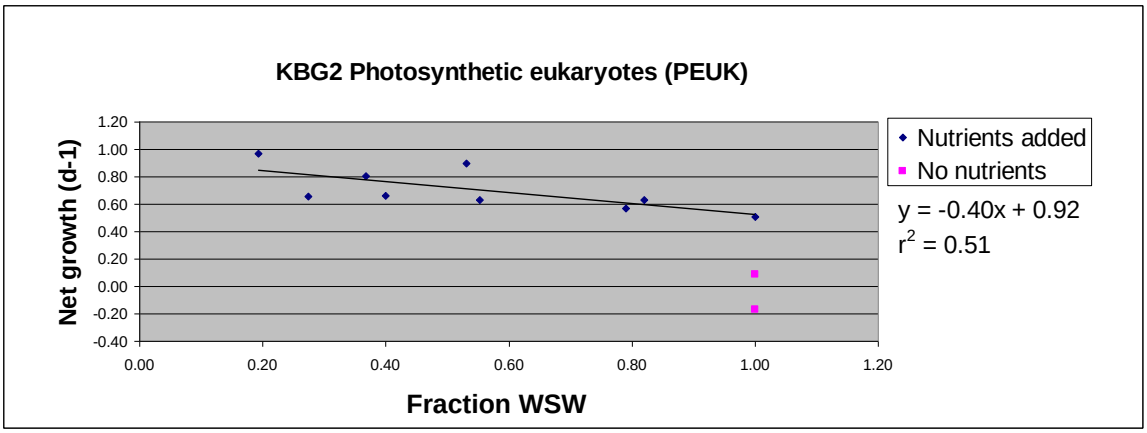

Figure 9C. KBG2 PEUK FCM, dilution factor vs. net growth per day.

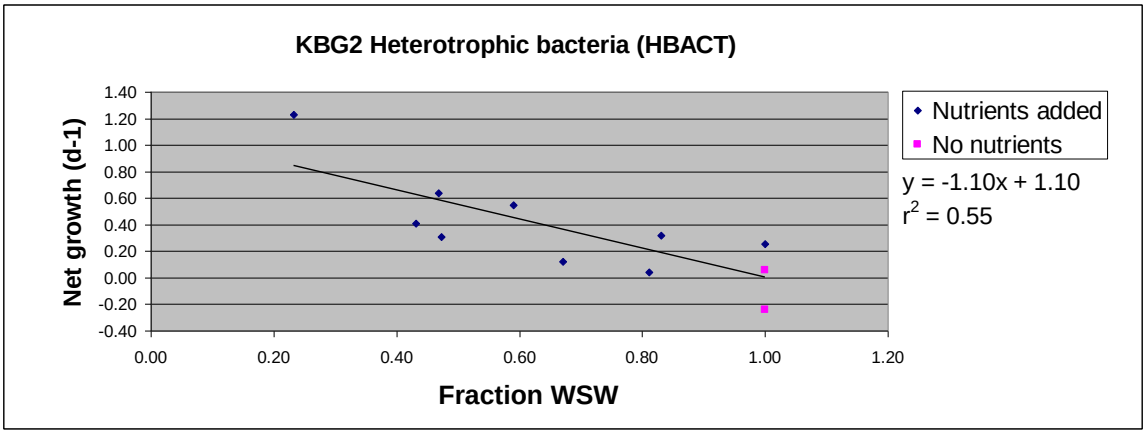

Figure 9D. KBG2 HBACT FCM, dilution factor vs. net growth per day.

Table 4. Growth and grazing rate data KBG1 and KBG2. The four populations shown are *Prochlorococcus* (PRO), *Synechococcus* (SYN), photosynthetic eukaryotes (PEUK) and heterotrophic bacteria (HBACT). Shown are the daily net growth rates, k, in experimental bottles without nutrients added (k_0), the growth rates with (μ_N) and without nutrients added (μ_0), as well as the microzooplankton mortality rates (m) for each population. The coefficient of determination (r^2) for each regression line from **Figures 8 and 9** is also shown.

Expt.	KBG1					KBG2				
Rates	k_0	μ_N	m	μ_0	r^2	k_0	μ_N	m	μ_0	r^2
PRO	**0.33**	**1.30**	**1.10**	**1.43**	**0.92**	**-0.47**	**0.69**	**0.84**	**0.37**	**0.64**
SYN	**0.43**	**1.30**	**1.10**	**1.53**	**0.80**	**-0.29**	**0.63**	**0.72**	**0.43**	**0.68**
PEUK	**0.46**	**1.26**	**0.94**	**1.40**	**0.79**	**-0.04**	**0.92**	**0.40**	**0.36**	**0.51**
HBACT	**0.27**	**1.15**	**1.03**	**1.30**	**0.94**	**-0.09**	**1.10**	**1.10**	**1.01**	**0.55**

KBG1 represents data from storm conditions for March 16-17, 2012. (See **Tables 2A and 2B** in the Methods section for precipitation data indicating storm and non-storm conditions.)

3.3.2. Percent phytoplankton growth consumed by grazers

For the storm-influenced experiment, KBG1, all phytoplankton populations were growing at a rate exceeding 1.30 d^{-1} (μ_0 ranged from 1.30 – 1.53 d^{-1}, **Table 4**), whereas for the non-storm influenced experiment phytoplankton were growing at a slower rate (μ_0 ranged from 0.36 – 1.01 d^{-1}, **Table 4**). Heterotrophic bacteria (μ_0) grew at a lower rate than the other 3 populations in the storm-influenced KBG1, at 1.30 d^{-1}, while in the non-storm-influenced KBG2, we observed a much higher growth rate for HBACT than the other 3 populations, at 1.01 d^{-1}.

Microzooplankton grazing did not balance growth for the KBG1 experiment, with only 83% on average of daily growth consumed (75-90% for all populations with added nutrients, **Table 5**). For KBG1 samples without added nutrients, the average for the percent grazed per day was 74% (a range of 67-79%, with photosynthetic eukaryotes as the lowest rate and heterotrophic bacteria at the highest). In contrast, mortality (grazing) exceeded growth in KBG2 with added nutrients for all populations except photosynthetic eukaryotes (43%). *Prochlorococcus, Synechococcus* and heterotrophic bacteria had an average 112% grazed per day, with a range of 100-122%. For KBG2 populations without added nutrients, mortality exceeded growth. The picoplankton populations PRO and SYN had particularly high percentages of grazing mortality (m/u_0) at 227% and 167% per day, respectively, but mortality roughly balanced growth ($m=\mu$) for the HBACT population, at 109% grazed per day. For the larger nanoplanktonic PEUK population, growth slightly

exceeded mortality, at 112% per day. With the exception of KBG2 PEUK at 43% growth grazed per day, all other KBG2 populations, including nutrient-amended and no-nutrients-added populations, showed mortality in excess of 100% growth grazed per day.

Table 5. Percent phytoplankton grazed ((m/μ)*100) on a daily basis, where m and μ are d^{-1}.

	Bottles 1-10, with added nutrients (m/u_n)		**Bottles 11-12, with no added nutrients (m/u_0)**	
Expt.	**KBG1**	**KBG2**	**KBG1**	**KBG2**
PRO	**0.85**	**1.22**	**0.77**	**2.27**
SYN	**0.85**	**1.14**	**0.72**	**1.67**
PEUK	**0.75**	**0.43**	**0.67**	**1.12**
HBACT	**0.90**	**1.00**	**0.79**	**1.09**
average	**0.83**	**0.95**	**0.74**	**1.54**

3.3.3. Comparison of phytoplankton growth rates with (μ_N) and without nutrients added (μ_0)

In comparing the effect of adding nutrients (versus not adding nutrients) between the two experiments conducted, we see little effect on growth rates of adding nutrients to the incubation bottles for the storm-influenced community in KBG1, whereas we see a great effect on growth rates in all populations of adding nutrients to the non-storm influenced microbial community during the KBG2 experiment. For instance, we observed a slight depression in growth rate with the nutrient-added treatment for all 4 populations (nutrient-amended growth rates are 85-91% of growth rates without added nutrients), with an average decrease in gross growth rate of 89% (**Table 6**, below). In contrast, during KBG2, the non-storm experiment, we see a positive nutrient affect on growth rate, ranging from an increase of 109 to 257% of nutrient-amended growth relative to no nutrients added, with the average percent increase in growth rate at 175%.

The HBACT population in KBG2 was least affected by the addition of nutrients, although it still was increased somewhat (109%). The PEUK population showed the biggest effect from added nutrients with an increase in nutrient-amended growth over 2.5-fold (257%).

Table 6. KBG1 and KBG2 nutrient effects ($(\mu_N/\mu_0)*100$) on growth rates.

Expt.	KBG1	KBG2	KBG2/KBG1
PRO	**91**	**187**	**205**
SYN	**85**	**147**	**172**
PEUK	**30**	**257**	**286**
HBACT	**88**	**109**	**124**
average	**89**	**175**	**197**

When comparing KBG2/KBG1 ratios of (μ_N/μ_0), PEUK showed the largest effect of added nutrients, growing nearly 3-times as fast (μ_N/μ_0= 2.86),, while HBACT showed the least effect (μ_N/μ_0= 1.24). The range of data for KBG2/KBG1 was an increase in growth with nutrients in KBG2 of 1.24 – 2.86, with an average of an ~2-fold increase in growth.

3.3.4. Doubling rates, in hours

The doubling rates (hours) in **Table 7** (below) show how long it took each population to double its abundance. For example, when comparing the nutrient-amended data for PRO KBG1, we observed PRO doubled its abundance in 12.7 hours. For PRO KBG2, its population took exactly 24 hours to double its abundance. For the no-nutrients-added (μ_0) comparison of PRO, we calculated that it took PRO only 11.6 hours to double its abundance in KBG1 storm conditions. For KBG2 (μ_0), it took PRO 44.8 hours to double its abundance. This means that without nutrients added but in storm conditions,

PRO was still able to double its abundance in less than one day, while it took almost 2 days to double its abundance in the non-storm conditions.

Table 7. Doubling rates (DT, hours) with (+Nuts) and without (-Nuts) added nutrients.

Expt.	KBG1		KBG2	
	DT+Nuts	DT-Nuts	DT+Nuts	DT-Nuts
PRO	12.7	11.6	24.0	44.8
SYN	12.7	10.8	26.3	38.5
PEUK	13.1	11.8	18.0	46.2
HBACT	14.4	12.7	15.1	16.4

The microbial community did not respond to added nutrients several days after the storm already input nutrients to the system, as indicated by the doubling rate compared between the no nutrient-added (11.6 hours) and the nutrient-added rate (12.7 hours). However, if we compare the effects on *Prochlorococcus* of being without added nutrients soon after a storm has passed (11.6 hours) versus non-storm conditions, during non-storm conditions, *Prochlorococcus* grew much slower, with a doubling rate of nearly 2 days (44.8 hours).

We can also compare the difference in one set of weather conditions for nutrient-amended versus no-nutrients-added to examine the difference in doubling rates. In KBG2, if we compare nutrient-amended (μ_N) to no-nutrients-added (μ_0), we see that having adding nutrients in non-storm (nutrient-depleted) conditions made a significant difference. For PRO, it took 24 hours for the nutrient-amended population to double its abundance; for no-nutrients-added, it took almost twice as long (44.8 hours) to double its abundance.

Data for SYN were roughly similar in trends to PRO. For KBG1, the nutrient-added (μ_N) rate (12.7 hours) was slightly less than half of the doubling rate of KBG2

nutrient-added rate of 26.3 hours. Samples from KBG1 for the no-nutrients-added (μ_0) showed that it took SYN only 10.8 hours to double its abundance in KBG1 storm conditions; however, in KBG2 non-storm conditions, it took nearly 4 times longer to double its abundance, at 38. 5 hours.

When comparing the nutrient-added (μ_N) doubling rate to the no-nutrients-added (μ_0) doubling rate within one set of weather conditions, we found that SYN in KBG1 nutrient-added (μ_N) population took 12.7 hours to double its abundance. KBG1 no-nutrients-added (μ_0) doubling rate was very slightly less, at 10.8 hours. There was almost no difference in these samples for storm conditions whether we added nutrients or not. For KBG2, we found the nutrient-added (μ_N) doubling rate was 26.3 hours; for the no-nutrients-added (μ_0) doubling rate, 38.5 hours. This was about half the difference in doubling rate that PRO displayed.

When comparing PEUK populations for the nutrient-added (μ_N) samples in both conditions, we found that PEUK doubled in 13.1 hours in KBG1, and took only slightly longer to double its abundance in KBG2, at 18.0 hours. Looking at the no-nutrients-added (μ_0) data, we saw a large difference comparable to that of PRO populations. PEUK (μ_0) for KBG1 doubled in 11.8 hours, while in KBG2, it took more than 4 times longer to double, at 46.2 hours, so PRO and PEUK showed some similarities in this respect.

When comparing the nutrient-added (μ_N) doubling rate to the no-nutrients-added (μ_0) doubling rate within one set of weather conditions, we found that PEUK in KBG1 nutrient-added (μ_N) population took 13.1 hours to double, versus 11.8 hours for the no-nutrients-added (μ_0). There was almost no difference in these samples for storm conditions whether we added nutrients or not. For KBG2, we found the nutrient-added

(μ_N) doubling rate was 18.0 hours, versus the no-nutrients-added (μ_0) doubling rate of 46.2 hours. This was the largest difference within one set of weather conditions per population of all populations measured.

When comparing HBACT populations for the nutrient-added (μ_N) samples in both conditions, it took KBG1 14.4 hours to double its abundance, versus 15.1 hours in KBG2, showing almost no difference from storm to non-storm conditions. Comparing the no-nutrients-added (μ_0) data, HBACT doubled its abundance in KGB1 in 12.7 hours, versus 16.4 hours in KBG2. Again, HBACT displayed the least amount of difference in this comparison than all other populations.

When comparing the nutrient-added (μ_N) doubling rate to the no-nutrients-added (μ_0) doubling rate within one set of weather conditions, we found that HBACT in KBG1 nutrient-added (μ_N) population took 14.4 hours to double, versus 12.7 hours for the no-nutrients-added (μ_0). HBACT displayed an average amount of difference in this compared to all other populations (PRO showed the least difference at 1.1 hours, while SYN showed the largest difference at 1.9 hours). For KBG2, we found the nutrient-added (μ_N) doubling rate was 15.1 hours, versus the no-nutrients-added (μ_0) doubling rate of 16.4 hours. HBACT showed the least difference in this category for KBG2 than all the other KBG2 populations (PEUK showed the largest difference, at 28.2 hours, while HBACT showed the least difference, at 1.3 hours).

3.3.5. Grazing rates (m = mortality) compared between KBG1 and KBG2

Grazing rates (mortality = m) were obtained from the FCM graph equations in **Figures 8 and 9** for each respective species. For KBG1, grazing rates were: for PRO and

SYN, 1.10 d^{-1}; for PEUK, 0.94 d^{-1}; for HBACT, 1.03 d^{-1}. For KBG2, grazing rates were: PRO, 0.84 d^{-1}; SYN, 0.72 d^{-1}; PEUK, 0.40 d^{-1}; HBACT, 1.10 d^{-1}.

For KBG2 (non-storm), grazing rates were generally lower than KBG1, except in the case of the heterotrophic bacteria, where KBG2 mortality rate was 1.10 d^{-1} compared to KBG1 mortality rate of 1.03 d^{-1}. For KBG1, *Prochlorococcus* had a mortality rate of 1.10 d^{-1}, compared the lower KBG2 mortality rate of 0.84 d^{-1}. For KBG1, *Synechococcus* mortality rate was 1.10 d^{-1}, compared to the lower KBG2 rate of 0.72 d^{-1}.

Photosynthetic eukaryotes showed the largest difference in grazing rates between KBG1 and KBG2: KBG2 was 0.40 d^{-1}, less than half its mortality rate of KBG1, at 0.94 d^{-1}.

Heterotrophic bacteria mortality rates showed the least difference from storm to non-storm conditions. As stated above, KBG1 mortality rate was 1.03 d^{-1}, compared to 1.10 d^{-1} for KBG2.

3.4. Chlorophyll

The chlorophyll (µg/L) measurements presented for the KBG1 and KBG2 experiments grazing represent a sum of chlorophyll and phaeopigment values. This was to compensate for the fact that all chlorophyll samples for all experiments were degraded during storage, and makes the assumption that all phaeopigment was originally derived from phytoplankton. Therefore, the values listed likely overestimate the amount of chlorophyll present. (For chlorophyll data on KBG1 and KBG2, see **Table 8, below.**)

Table 8. Fluorometric chlorophyll-a data from KBG1 and KBG2.

Expmt.	Sample No	Dilution Factor	Chl a (µg/L)	Phaeo (µg/L)	TOTAL (Chl+Phaeo)
KBG1	**Initial-1**	10	0.20	1.02	1.22
	Initial-2	10	0.18	0.91	1.08
average			**0.19**	**0.96**	**1.15**
	Final-1	10	0.09	0.43	0.52
	Final-2	10	0.09	0.40	0.50
	Final-3	20	0.15	0.57	0.72
	Final-4	10	0.15	0.82	0.97
	Final-5	10	0.28	1.31	1.58
	Final-6	10	0.23	1.30	1.53
	Final-7	10	0.38	1.68	2.06
	Final-8	10	0.43	1.85	2.28
	Final-9	20	0.45	1.60	2.06
	Final-10	20	0.30	1.42	1.72
	Final-11	20	0.12	0.66	0.79
	Final-12	20	0.16	0.73	0.89
	Final-13	0	0.00	0.00	0.00
KBG2	**Initial-1**	10	0.13	0.65	0.78
	Initial-2	10	0.13	0.60	0.72
	Initial-3	10	0.13	0.51	0.64
average			**0.13**	**0.59**	**0.71**
	Final-1	10	0.07	0.29	0.36
	Final-2	10	0.07	0.28	0.35
	Final-3	10	0.13	0.51	0.64
	Final-4	10	0.14	0.55	0.69
	Final-5	10	0.23	0.91	1.14
	Final-6	10	0.20	1.02	1.22
	Final-7	10	0.88	0.37	1.25
	Final-8	10	0.35	1.45	1.81
	Final-9	20	0.35	1.70	2.06
	Final-10	20	0.35	1.81	2.17
	Final-11	10	0.09	0.40	0.49
	Final-12	10	0.09	0.38	0.47

We analyzed 2 initial samples for KBG1. Chlorophyll-a showed a range from 0.18-0.20 µg/L. Phaeopigment showed a range of 0.91-1.02 µg/L, with an average of 0.96 µg/L. For chlorophyll-a plus phaeopigment, there was a range from 1.08-1.22 µg/L, with an average of 1.15 µg/L. We analyzed 3 initial samples for KBG2. Chlorophyll-a showed were identical, all at 0.13 µg/L. Phaeopigment showed a range of 0.51-0.65 µg/L, with an average of 0.59 µg/L. For chlorophyll-a plus phaeopigment, there was a range from 0.64-0.78 µg/L, with an average of 0.71 µg/L. We can see by comparison that all data were higher for the initials of KBG1 than for the initials of KBG2. Because our samples were all degraded during storage, as mentioned above, we are using these data only for qualitative purposes to show that chlorophyll-a was likely much higher in KBG1 than KBG2.

There was not much difference between KBG1 initials and finals, with chlorophyll plus phaeopigment averages at 1.15 µg/L initial versus 1.20 µg/L final. There was a larger difference between KBG2 initials and finals, with chlorophyll plus phaeopigment averages at 0.71 µg/L initial versus 1.05 µg/L final.

For KBG2, *Prochlorococcus* and *Synechococcus* populations had much dimmer chlorophyll fluorescence/cell measurements with flow cytometry than their KBG1 counterparts.

4. DISCUSSION

4.1. Microbial community dynamics

4.1.1. Microplankton biomass and abundance

Barber and Hiscock (2006) observed that during a storm event, the smaller cells such the picoplankton (PRO and SYN) showed only a modest increase in biomass and abundance. This is due to the fact that while phytoplankton are increasing their biomass and abundance, so are all the grazers, and thus the grazers consume phytoplankton at a constant rate, making it appear as though the smaller cells have less biomass and abundance than their larger cell counterparts. If smaller-celled organisms appear less dominant in terms of biomass and abundance during a storm (Hoover, 2006), this is factoring in that grazers are consuming these smaller populations as fast as they are growing. Diatoms, on the other hand, grow rapidly during a bloom and are bigger, allowing many of them to escape grazing control, and so they dominate the bloom, with much more biomass than the smaller cells.

According to our flow cytometry data, PRO and SYN did show only a modest increase in biomass and abundance during a storm, so this agrees with Barber and Hiscock's (2006) and Hoover's (2006) results. In fact, PRO did not show much difference in biomass and abundance between either storm versus non-storm conditions, but there was slightly more variability in non-storm conditions.

Our data for SYN also agreed with Barber and Hiscock (2006) and Hoover's (2006) results. SYN did show a modest increase in biomass and abundance during storm conditions, and both categories were higher in KBG2 than KBG1. This suggests that the smaller-celled organisms are more successful in dominating the biomass structure when nutrients are depleted. It may also suggest that diatoms are not as successful during non-

storm conditions, but thrive during storm conditions and dominate more of the autotrophic biomass.

HBACT did not show significant differences between storm and non-storm in either biomass or abundance. This could indicate that HBACT are not limited in abundance by nutrients introduced through storms, and that their populations are regulated by other factors.

The general trend for autotrophs in KBG1 and KBG2 for particles ranging from the 2-20 µm range was moderate increases in biomass and significantly larger increases in abundance. For KBG1, the >20.1 µm category showed a larger increase in biomass than abundance, and followed the same trend to a lesser degree in KBG2. For diatoms, both biomass and abundance were higher in KBG1 than in KBG2. This could indicate the diatom dominance during storm conditions and agrees with Hoover's (2006) research. The general trend for heterotrophs in KBG1 showed a modest increase in biomass and a slightly higher increase in abundance for the size ranges 2-20 µm. For the >20.1 µm size category, a huge increase of almost 300x more than the 2-20 µm was evident in biomass. While the abundance was the highest of all 4 heterotroph size categories, it was more within the range of increase presented in the other size categories, with a range of 1-13 µm. KBG2 showed the same pattern for the 5-20 µm categories: a modest increase during non-storm conditions and only slight abundance increase. The >20.1 µm category showed a 5x increase in biomass compared to the 5-20 µm range data, and the abundance data for the >20.1 µm set was within the same small range of increase as its 5-20 µm counterparts. All of the above agrees with the research trends of Hoover (2006) and Barber and Hiscock (2006) in that larger cells appear to gain dominance during storm

conditions, whereas smaller cells gain dominance during non-storm conditions. One anomaly was there were no heterotrophs found in the 2-5 µm size category for KBG2. This goes against the researchers' results just mentioned because smaller cells are known to thrive in nutrient-depleted conditions. Possible causes of this absence of cells could be due to selective predation of this size category by larger predators such as microzooplankton. Because we analyzed only the large volume slides in this experiment, it is also possible that we underestimated the smaller cells populations. The large volume slides were filtered through an 8 µm size black polycarbonate filter, which allowed smaller particles to pass through it. Had we also analyzed the smaller volume slides (the samples of which were passed through an 0.8 µm size black polycarbonate filter), it is likely that a higher abundance of smaller cells would be revealed.

4.1.2. Chlorophyll

Storm events and their resulting blooms occur rapidly in Kaneohe Bay and are on the scale of days to weeks (Drupp, 2011). Chlorophyll levels rise over the course of this event, indicating the increasing abundance and biomass of phytoplankton. Our initial chlorophyll samples were within the range of Drupp (2011) records for the South Bay station in Kaneohe Bay (average corrected initial: 1.15 µg Chl/L). Drupp's chlorophyll-a concentrations for winter in the South Bay were 1.91 ± 1.51 µg Chl/L, range 0.22 – 7.87 µg Chl/L. Winter is when most storms occur, which correlates to our KBG1 storm conditions, despite our sampling being in March. Our data for KBG1 showed a chlorophyll-a concentration of 1.15 µg/L. One possible reason our values were lower than Drupp's could be that we missed the peak chlorophyll production time, which would have occurred ~5 days after the storm (Hoover, 2006); we collected our storm condition

samples ~10 days after the peak of the storm (although we continued to have rainshowers right up to the date of sample collection). This can be seen in **Figure 4**.

For summer, Drupp's data showed 0.48 ± 0.28 µg Chl/L, range 0.07-0.94 µg Chl/L. These data are within the range of our non-storm conditions of KBG2 (average corrected initial 0.71 µg Chl/L). As explained by Hoover (2006), phytoplankton, as measured by their chlorophyll content, continue to show storm-effects on growth over a period of weeks, albeit at a slower rate than at the beginning of storm conditions. Thus, it could be that the phytoplankton community sampled during non-storm conditions was still being influenced by prior bloom conditions lingering from the March 5 storm. For our non-storm sampling date, our weather conditions showed minor rainshowers up until 2 days before collection time, so our increased concentration of chlorophyll-a could also be the ongoing response of the phytoplankton to small amounts of nutrient runoff from streams.

4.2. Phytoplankton growth rates in storm vs. non-storm conditions

We observed a large difference in growth rates between storm and non-storm conditions in the no-nutrients-added category (μ_0), as shown in **Table 4**, for all populations. KBG2 PRO had a growth rate of 0.37 d^{-1}, compared to KBG1 PRO, at 1.43 d^{-1}. SYN followed the same pattern, with a growth rate of 0.43 d^{-1} for KBG2 and 1.53 d^{-1} for KBG1. KBG2 PEUK continued the trend, with a growth rate of 0.33 d^{-1}, compared to KBG1 PRO, at 1.40 d^{-1}. What is interesting to note about this large growth rate of the smaller cells is that, like the larger cells such as diatoms, they did benefit from storm conditions. Benefits were not solely the domain of the largest cells. All populations were

growing at ~0.3-0.4 d-1 under non-storm and then all populations increased their growth rates dramatically to 1.4-1.5 d-1 under storm conditions.

Even HBACT showed an effect of increased nutrients, with a growth rate of 1.01 d^{-1} during KBG2 compared to KBG1 at 1.30 d^{-1}. However, during KBG2, this population showed the least increase with added nutrients, which indicates that this population thrived in nutrient-stressed conditions as well as nutrient-replete conditions, as both growth rates were high.

With regard to net growth rates, the growth rate k_0 as viewed in **Table 4** shows KBG2 non-storm conditions had negative growth rates (average -0.22 d^{-1}), whereas KBG1 storm conditions had slightly positive growth rates (average 0.37 d^{-1}).

The graphs of phytoplankton net growth rate as a function of dilution factor (**Figures 8 and 9**) reveal differences in net growth per day based on dilution factors and whether or not nutrients were added to the experimental bottles. The more diluted the sample, the fewer grazers were included, which meant that phytoplankton net growth was less hindered by grazing, and so it increases with dilution level (i.e., $k = \mu - m$, where m decreases but μ does not).

The difference nutrients made to net growth rates were varied. All phytoplankton populations showed slightly lower growth (~10%) when nutrients were added in KBG1. Data points for the no-nutrients samples appeared roughly along and slightly above the continuum of the trendline for phytoplankton growth, indicating slightly lower growth (~10%) when nutrients were added in KBG1. For KBG2, however, we saw a different pattern. The data points in **Figure 9** for the no-nutrients-added samples showed significantly lower net growth rates appear below the continuum of the trendline,

indicating that all populations displayed dramatic increases in growth (from ~50-150%) with added nutrients. KBG2 PEUK showed this effect the most (increase in growth 2.5-fold): both no-nutrient net growth rates appeared well below the trendline, indicating a much slower growth rate than their nutrient-amended counterparts. Thus, nutrients added in non-storm conditions provided nutrient-stressed populations with fuel to boost their primary production.

Daily net growth rates (**Table 4**) show that all 4 KBG2 populations had a negative net growth rate of range -0.04 to -0.47 d^{-1}. All 4 KBG1 populations had a positive net growth of range 0.27 to 0.46 d^{-1}. This supports the trends described above, in which >100% growth grazed meant a net decrease for the nutrient-stressed non-storm conditions, and a <100% grazed in KBG1 supports our evidence that a positive net growth occurred.

4.2.1. Doubling times

Doubling times show how many hours it took for a population to double its abundance. The data show that all phytoplankton populations were growing quite fast. As evident in **Table 7**, KBG1 doubling times were all under 24 hours, regardless of whether or not we added nutrients. Even in KBG2, the longest doubling time (PEUK, no added nutrients) was still under 2 days, at 46.2 hours. In **Table 7**, we compared KBG1 and KBG2, each with nutrients-added and no-nutrients-added categories. What we found was that during storm conditions, it made little difference in doubling time whether or not we added nutrients artificially. This supports our growth and grazing data from **Table 4**, which also showed that adding nutrients to already nutrient-replete storm conditions

provided little benefit to phytoplankton, which were already utilizing nutrients and growing at their maximum rate.

For KBG2, with the exception of HBACT in **Table 4,** in which this population showed almost no effect of adding nutrients, the other 3 populations all showed increased growth rates when adding nutrients to non-storm condition samples. This was reflected in significantly lower doubling times for the nutrient-amended samples in non-storm conditions. Particularly affected were PRO and PEUK populations, where doubling times took 2-3x longer without nutrients than with nutrients.

4.3. Phytoplankton mortality during storm vs. non-storm conditions

For the no-nutrients-added samples (μ_0) for all 4 populations sampled, an average of 74% of phytoplankton was consumed by grazers in KBG1 versus an average of 154% consumed in KBG2 (**Table 5**). This means that during the storm conditions of KBG1, grazers were not able to consume all the phytoplankton at the rate at which the phytoplankton were growing. In other words, phytoplankton growth exceeded mortality effects from grazers. Since excess growth over grazing is the definition of a phytoplankton bloom, this indicates that a phytoplankton bloom was occurring, potentially as a result of the nutrients added to the site by runoff immediately following the early-March storms. For KBG2, experiment conducted under non-storm conditions, grazers consumed phytoplankton at a rate much faster than the phytoplankton could grow. Under non-storm conditions, there were no excess added nutrients from stream and land runoff; therefore, phytoplankton abundance in this experiment was limited by available nutrients and their growth was controlled by grazing.

We added nutrients (μ_N) to the already nutrient-replete samples from KBG1 storm conditions, and found there was little effect on phytoplankton growth rate– indeed the growth rate in the nutrient-amended samples was somewhat lower than that in the un-amended samples (**Table 4**). This is because phytoplankton were already experiencing optimal nutrient supply and were growing at their maximum possible rate. The nutrients we added were excess and our experimental evidence showed that they had little to no effect on growth; it appears the added nutrients were not utilized. On average for all 4 populations, 83% of phytoplankton growth was grazed for KBG1 when no nutrients were added versus a slightly lower 74% of phytoplankton mortality for KBG1 without added nutrients, demonstrating the weak negative effect of adding nutrients artificially. (**Table 5**). Thus, at the time of our KBG1 storm sample collection, nutrients had apparently been provided to the microbial community by a combination of stream runoff and mixing of vertical layers from storm turbidity and wind forcing.

There are a few standout percentages worth mentioning, such as a low for PEUK for KBG2 of 43% grazed relative to growth in the nutrient-added category (the other 3 populations were all 100% or greater). Under non-nutrient amended conditions, PEUK mostly represent phytoplankton that belong to the nanoplankton size category (2-20 µm): however with nutrients added, the much higher growth rate (μ_N = 0.92 d^{-1} vs. μ_0 = 0.36 d^{-1}) probably represents a growth of diatoms in the experimental treatments which were able to escape grazer control.

There were relative high rates of 227% and 167% phytoplankton mortality relative to growth for PRO and SYN in the no-nutrients-added KBG2 (the other 2 populations were ~110%). PRO and SYN belong to the picoplankton size category of

0.2-2 µm and as mentioned in the introduction, Hoover (2006) reported a dominance of smaller cells during non-storm conditions. This is because the smaller cells are more efficient and can utilize much lower nutrient concentrations than their larger counterparts, nano and micro-zooplankton (2-200 µm). Hoover (2006) also noted that as the storm and bloom conditions progressed, a gradual shift in dominance from smaller to larger cells occurred during storm conditions. We observed this as well, as indicated by our biomass data.

5. CONCLUSIONS

Our research results largely agreed with the prior results of Hoover (2006), in terms of the composition of phytoplankton in storm vs. non-storm conditions. For example, the typical composition of storm samples we analyzed showed dominance by larger cells, specifically chain-forming diatoms. The non-storm conditions samples showed that smaller cells such as picoplankton (SYN) dominated. Using flow cytometry, we analyzed the effects of artificially adding nutrients to both storm and non-storm conditions, as well as examining non-nutrient-amended samples. When nutrient conditions were optimal in storm conditions, our addition of nutrients did not enhance growth; in fact, it slowed the doubling rates slightly, as in KBG1 PRO, where non-nutrient-amended samples took 11.6 hours to double, but took 12.7 hours to double when nutrients were artificially added. We found that growth exceeded grazing in storm conditions, which led to algal blooms. Grazers consumed an average of 83% of phytoplankton growth; therefore, net phytoplankton growth rate was positive. In non-storm conditions, we found that grazing exceeded growth, where grazing was 112%, and caused a negative net phytoplankton growth rate.

Understanding the grazing behaviors of microzooplankton may indicate how availability is quantified for the top ten percent of the food web. That is, based on the efficiency of energy transfer from primary producers and primary consumers (phytoplankton and microzooplankton, respectively) upward to top predators, grazing at microbial levels may dictate the success or failure of higher trophic levels, a valuable marine resource. From our results, during non-storm conditions, virtually all the primary production was consumed by the smallest grazers, the microzooplankton, leaving little

primary production to be consumed directly by larger grazers. Under storm-conditions, however, some fraction of the phytoplankton escaped grazing by microzooplankton, and therefore could be available for direct consumption by larger zooplankton grazers. In the latter situation, more primary production could be funneled to higher trophic levels, thus increasing the resources available to them. However, more research on the fate of the excess phytoplankton production generated during storm-conditions needs to be done to determine whether this scenario occurs.

6. APPENDIX A: TABLES

Table A1. Picoplankton abundance and rate data from flow cytometry samples taken during KBG1 and KBG2 experiments conducted in Kaneohe Bay.

Expmt.	Bottle #	Pro/ml initial	Pro/ml final	Pro Dilution Factor	Pro k (d-1)	Bottle #	Syn/ml initial	Syn/ml final	Syn Dilution Factor	Syn k (d-1)
KBG 1	1	36142	118590	0.17	1.19	1	36393	104178	0.21	1.05
	2	41581	111470	0.20	0.99	2	38233	99321	0.22	0.95
	3	77816	90123	0.37	0.15	3	68009	82911	0.40	0.20
	4	78266	178196	0.37	0.82	4	68380	156280	0.40	0.83
	5	115784	238569	0.55	0.72	5	99890	210010	0.59	0.74
	6	118219	236346	0.56	0.69	6	100195	209719	0.59	0.74
	7	168416	288236	0.80	0.54	7	144065	248389	0.84	0.54
	8	170374	280931	0.81	0.50	8	140174	252438	0.82	0.59
	9	208925	255231	1.00	0.20	9	171327	219962	1.00	0.25
	10	208422	201196	1.00	-0.04	10	174980	149399	1.00	-0.16
	11	209137	250374	1.00	0.18	11	160555	234652	1.00	0.38
	12	214272	343978	1.00	0.47	12	175430	283154	1.00	0.48
KBG 2	1	47631	89289	0.20	0.63	1	57816	99107	0.23	0.54
	2	47723	93581	0.20	0.67	2	57068	103373	0.22	0.59
	3	91888	124688	0.38	0.31	3	105263	158931	0.41	0.41
	4	110762	126381	0.46	0.13	4	109358	115999	0.43	0.06
	5	143194	186874	0.60	0.27	5	154731	196219	0.60	0.24
	6	140346	136461	0.59	-0.03	6	153234	159206	0.60	0.04
	7	200117	236014	0.83	0.16	7	213557	244742	0.83	0.14
	8	197741	151410	0.82	-0.27	8	219844	201744	0.86	-0.09
	9	237208	*	1.00	*	9	269378	*	1.00	*
	10	248115	259727	1.00	0.05	10	264246	267866	1.00	0.01
	11	216878	114138	1.00	-0.64	11	236749	147881	1.00	-0.47
	12	257368	190824	1.00	-0.30	12	253457	227141	1.00	-0.11

*No data returned due to possible clog in flow cytometer. See section 3.2 for explanation.

Table A1. (CONTINUED)
Picoplankton abundance and rate data from flow cytometry samples taken during KBG1 and KBG2 experiments conducted in Kaneohe Bay.

Expmt.	Bottle #	Peuk/ml initial	Peuk/ml final	Peuk Dilution Factor	Peuk k (d-1)	Bottle #	Hbact/ml initial	Hbact/ml final	Hbact Dilution Factor	Hbact k (d-1)
KBG 1	**1**	7265	16212	0.26	0.80	**1**	339942	851859	0.24	0.92
	2	5545	16781	0.20	1.11	**2**	328904	832471	0.23	0.93
	3	11024	13777	0.39	0.22	**3**	580999	716290	0.41	0.21
	4	10336	25198	0.37	0.89	**4**	559401	1095748	0.39	0.67
	5	14452	37254	0.52	0.95	**5**	842621	1482233	0.59	0.56
	6	15590	32781	0.56	0.74	**6**	834099	1474359	0.58	0.57
	7	21849	42984	0.78	0.68	**7**	1202467	1644561	0.84	0.31
	8	21585	40853	0.77	0.64	**8**	1152945	1673637	0.81	0.37
	9	27963	38908	1.00	0.33	**9**	1439117	1818708	1.00	0.23
	10	31801	34170	1.00	0.07	**10**	1491550	1424904	1.00	-0.05
	11	26666	38140	1.00	0.36	**11**	1294245	1725183	1.00	0.29
	12	25753	45432	1.00	0.57	**12**	1484285	1909585	1.00	0.25
KBG 2	**1**	3163	6103	0.27	0.66	**1**	658009	990242	0.43	0.41
	2	2231	5880	0.19	0.97	**2**	354257	1211109	0.23	1.23
	3	4620	8964	0.40	0.66	**3**	721127	980372	0.47	0.31
	4	4253	9503	0.37	0.80	**4**	713685	1348463	0.47	0.64
	5	6143	15081	0.53	0.90	**5**	900546	1554564	0.59	0.55
	6	6392	12023	0.55	0.63	**6**	1023146	1157743	0.67	0.12
	7	9476	17771	0.82	0.63	**7**	1266510	1745481	0.83	0.32
	8	9135	16104	0.79	0.57	**8**	1237084	1289334	0.81	0.04
	9	9752	*	1.00	*	**9**	1575919	*	1.00	*
	10	11406	18953	1.00	0.51	**10**	1534824	1979732	1.00	0.25
	11	10973	11959	1.00	0.09	**11**	1419823	1114573	1.00	-0.24
	12	14109	11918	1.00	-0.17	**12**	1568516	1661126	1.00	0.06

*No data returned due to possible clog in flow cytometer. See section 3.2 for explanation

7. REFERENCES

Azam, F., Fenchel, T., Field, J.G., Gray, J.S., Meyer-Reil, L.A., Thingstad, F. 1983. The ecological role of water-column microbes in the sea. Marine ecology progress series, vol 10, January 20, 257-63.

Barber, R.T., Hiscock, M.R. 2006. A rising tide lifts all phytoplankton: growth response of other phytoplankton taxa in diatom-dominated blooms. Global biogeochemical cycles, vol 20, GB4S03, 1-12.

Burkill et al. 1987. Microzooplankton grazing and selectivity of phytoplankton in coastal waters. Marine Biology, vol 93, issue 4, 581-590.

Burkill, P.H., Leakey, R.J.G., Owens, N.J.P., Mantoura R.F.C. 1993. *Synechococcus* and its importance to the microbial food web of the northwestern Indian Ocean. Deep sea research part II: topical studies in oceanography, vol 40, issue 3, 773-782.

Calbet, A., Landry, M.R. 1999. Mesozooplankton influences on the microbial food web: direct and indirect trophic interactions in the oligotrophic open ocean. Limnology and oceanography, vol 44, 1370-80.

Calbet, A., Landry, M.R. 2004. Phytoplankton growth, microzooplankton grazing, and carbon cycling in marine systems. Limnology and Oceanography, vol 40, 51–57.

Christian, J.R., Karl, D.M. 1994. Microbial community structure at the US Joint Global Ocean Flux Study Station (JGOFS) ALOHA: inverse methods for estimating biochemical indicator ratios. Journal of geophysical research, vol 99, issue C7, 14,269-14,276.

DeCarlo, E.H., Hoover, D.J., Young, C.W., Hoover, R.S., Mackenzie. 2007. Impact of storm runoff from tropical watersheds on coastal water quality and productivity. Applied geochemistry, vol 22, 1777-97.

Drupp, P., De Carlo, E.H., Mackenzie, F.T., Bienfang, P., Sabine, C.L. 2011. Nutrient inputs, phytoplankton response, and CO2 variations in a semi-enclosed subtropical embayment, Kaneohe Bay, Hawaii. Aquatic geochemistry, vol 17, 473–498.

Eppley, R.W., Reid, F.M., Strickland, J.D.H. 1970. Estimates of phytoplankton crop size, growth rate, and primary production. The ecology of the plankton off La Jolla, California, in the period April through September (1967). Bulletin of Scripps Institute of Oceanography, vol 17, 33-42.

Fenchel, T. 2008. The microbial loop—25 years later. Journal of experimental marine biology and ecology, vol 366, 99-103.

Garrison, D.L., et al. 2000. Microbial food web structure in the Arabian sea: a US JGOFS study. Deep sea research, part II, vol 47, 1387-1422.

Hoover, R.S., Hoover, D., Miller, M., Landry, M.R., DeCarlo, E.H., Mackenzie, F.T. 2006. Zooplankton response to storm runoff in a tropical estuary: bottom-up and top-down controls. Marine ecology progress series, vol 318, 187-201.

Irigoien, X., Flynn, K.J., Harris, R.P., 2005. Phytoplankton blooms: a 'loophole' in microzooplankton grazing impact? Journal of Plankton Research, vol 27, 313–321.

Kamiyama, T. 1994. The impact of grazing by microzooplankton in northern Hiroshima Bay, the Seto Inland Sea, Japan. Marine Biology, vol 119, issue 1, 77-88.

Keys, A., Christensen, E.H., Krogh, A. 1935. The organic metabolism of sea-water with special reference to the ultimate food cycle in the sea. Journal of Marine Biology Association U.K., vol 20, 181–196.

Landry, M.R., Hassett, R.P. 1982. Estimating the grazing impact of marine micro-zooplankton. Marine biology, vol 67, 283-88.

Landry, M.R. 2002. Integrating classical and microbial food web concepts: evolving views from the open-ocean tropical Pacific. Hydrobiologia, vol 480, 29–39.

Landry, M.R., Kirchman, D.L. 2002. Microbial community structure and variability in the tropical Pacific. Deep-sea research, part II, vol 49, 2669-93.

Liu, H. and Dagg, M. 2003. Interactions between nutrients, phytoplankton growth, and micro- and mesozooplankton grazing in the plume of the Mississippi River. Marine Ecology Progress Series, vol 258, 31-42.

Massaro, R.F.S, De Carlo, E.H., Drupp, P.S., Mackenzie, F.T., Jones, S.M., Shamberger, K.E., Sabine, C.L., Feely, R.A. 2012. Multiple Factors driving variability of CO2 exchange between the ocean and atmosphere in a tropical coral reef environment. Aquatic geochemistry, vol 18, 357–386.

Mateo, I. 2007. A bioenergetics based comparison of growth conversion efficiency of Atlantic Cod on Georges Bank and in the Gulf of Maine. Journal of northwest Atlantic fishery science, vol 38, 23-35.

Menden-Deuer, S., Lessard, E.J. 2000. Carbon to volume relationships for dinoflagellates, diatoms and other protist plankton. Limnology and Oceanography, vol 45, issue 3, 569-79.

NOAA National Climatic Data Center's Quality Controlled Local Climatological Data. http://cdo.ncdc.noaa.gov/qclcd/QCLCD

Partensky, F., Hess, W.R., Vaulot, D. 1999. *Prochlorococcus,* a marine photosynthetic prokaryote of global significance. Microbiology and molecular biology reviews, vol 63, issue 1, 106-27.

Pomeroy, L.R. 1974. The oceanic food web, a changing paradigm. BioScience, vol 24, issue 9, September, 499-504.

Ringuet, S., Mackenzie, F.T. 2005. Controls on nutrient and phytoplankton dynamics by storm runoff events in southern Kaneohe Bay, Hawaii. Estuaries, vol 28, 327-37.

Selph, K.E., Shacat, J., Landry, M.R. 2005. Microbial community composition and growth rates in the NW Pacific during spring 2002. Geochemistry, Geophysics, Geosystems: an electronic journal of the earth sciences, vol 6, no 12, December.

Shalapyonok, A., Olson, R.J., Shalapyonok, L.S. 2001. Arabian sea phytoplankton during SW and NE monsoons 1995: composition, size structure and biomass from individual cell properties measured by flow cytometry. Deep sea research, part II, vol 48, 1231-61.

Sherr, E.B., Sherr, B.F. 1988. Role of microbes in pelagic food webs: a revised concept. Limnology and oceanography, vol 33, 1225-1227.

Sherr and Sherr. 1994. Bacterivory and herbivory: key roles of phagotrophic protists in pelagic food webs. Microbial ecology, vol 28, issue 2, 223-235.

Sherr, E.B., Sherr, B.F. 2002. Significance of predation by protists in aquatic microbial food webs. Antonie van Leeuwenhoek, vol 81, 293-308.

Sherr, E.B., Sherr, B.F., Hartz, A.J. 2009. Microzooplankton grazing impact in the Western Arctic Ocean. Deep sea research part II: topical studies in oceanography, vol 56, issue 17, 1 August, 1264-1273.

Siegel, D.L., Doney, S.C., Yoder, J.A. 2002. The North Atlantic spring phytoplankton bloom and Sverdrup's critical depth hypothesis. Science, vol 296, 730-33.

Smith, S.V., Kimmerer, W.J., Laws, E.A., Brock, R.E., Walsh, T.W. 1981. Kaneohe Bay sewage experiment: perspectives on ecosystem responses to nutritional perturbation. Pacific science, vol 35, 379-95.

Stoecker, D.K. 1998. Conceptual models of mixotrophy in planktonic protists and some ecological and evolutionary implications. European journal of protistology, vol 34, October 12, 281-90.

Straile, D. 1997. Gross growth efficiencies of protozoan and metazoan zooplankton and their dependence on food concentration, predator-prey weight ratio, and taxonomic group. Limnology and oceanography, vol 42, issue 6, 1375-85.

Sverdrup, H.U. 1953. Journal cons. Perm. Int. expl. Mer., vol 18, issue 287.

Throndsen, J. 1978. Preservation and storage. *Phytoplankton manual*, 69-74.